

# UNIVERSITY OF NAPLES “FEDERICO II”



**XXVII Cycle**

**PhD Program in Neuroscience**

**School of Molecular Medicine**

## **Na<sub>v</sub>1.6 As A New Potential Target In Alzheimer's Disease**

**Coordinator:  
Prof. Lucio Annunziato**

**Tutor:  
Prof. Anna Pannaccione**

**PhD Student:  
Cristina Franco**

**ACADEMIC YEAR 2014-2015**

## Summary

<b>1.INTRODUCTION</b> .....	4
1.1 Alzheimer's Disease.....	4
1.1.1 A $\beta$ Peptide And Amyloid Cascade Hypothesis .....	4
1.1.2 APP processing and A $\beta$ generation .....	6
1.1.3 A $\beta$ Affects Neuronal Excitability.....	10
1.1.4 Mouse Models Of Alzheimer's Disease .....	12
1.2 Intrinsic membrane proprieties of Neurons and Voltage Gated Na <sup>+</sup> Channels.....	15
1.2.1 Voltage Gated Na <sup>+</sup> Channels Structure .....	15
1.2.2 Sodium Channel Classification and Nomenclature .....	18
1.2.3 Voltage Gated Na <sup>+</sup> Channels Functional Expression.....	20
1.2.4 Types of Na <sub>v</sub> currents.....	21
1.2.5 Molecular basis of Na <sub>v</sub> currents.....	23
1.3 Na <sub>v</sub> 1.6 Sodium Channel.....	24
1.3.1 Unique Biophysical Properties Of Na <sub>v</sub> 1.6 .....	25
1.3.2 Regulative Protein Interactions Of Na <sub>v</sub> 1.6 .....	27
1.3.3 Na <sub>v</sub> 1.6 Role In Pathophysiological Conditions .....	32
1.4 Voltage-Gated Sodium Channels And Alzheimer's Disease.....	33
<b>2. AIM OF THE STUDY</b> .....	36
<b>3. MATERIALS AND METHODS</b> .....	37
3.1 Drugs And Chemicals .....	37
3.2 Mice .....	37
3.2.1 Genotyping: PCR Analysis.....	38
3.3 Mouse Hippocampal Cell Cultures.....	39
3.4 A $\beta$ Oligomers Preparation And Cellular Treatments .....	40
3.5 Anisomycin Treatment .....	40
3.6 Western-blot analysis.....	41
3.7 Electrophysiological recordings.....	42
3.8 Immunocytochemistry in hippocampal neurons .....	43

3.9 Na <sub>v</sub> 1.6 Silencing RNA Transfection.....	44
3.10 Statistical Analysis .....	45
<b>4. RESULTS</b> .....	<b>46</b>
4.1 A $\beta$ <sub>1-42</sub> exposure raised Na <sub>v</sub> functional activity in hippocampal neurons	46
4.2 A $\beta$ <sub>1-42</sub> fails to increase Na <sup>+</sup> currents in Na <sub>v</sub> 1.6 silenced mouse hippocampal cultures .....	47
4.3 pp38-mediated Internalization of Na <sub>v</sub> 1.6 counteracts A $\beta$ -induced I <sub>Na<sup>+</sup></sub> increase .....	49
4.4 Increased Na <sub>v</sub> activity in hippocampal neurons of AD mouse model Tg2576.....	49
4.5 The Anisomycin-stimulated Na <sub>v</sub> 1.6 Endocytosis Prevents Increase Of I <sub>Na<sup>+</sup></sub> Currents In Hippocampal Neurons Of Tg2576 Mice .....	51
4.6 I <sub>Na<sup>+</sup></sub> Increase Is Accompanied By An Overexpression of Na <sub>v</sub> 1.6 Channel Subunits In Tg2576 Hippocampal Neurons.....	52
4.7 Reduced Expression Of Na <sub>v</sub> $\beta$ 1 Auxiliary Subunit In Tg2576 Hippocampal Neurons .....	54
<b>5. DISCUSSION</b> .....	<b>56</b>
<b>6. REFERENCES</b> .....	<b>62</b>

# 1. INTRODUCTION

## 1.1 Alzheimer's Disease

Alzheimer's Disease (AD) is the most frequent neurodegenerative disorder and the most common cause of dementia in the elderly, that leads to severe memory loss and cognitive impairment. Current estimates suggests that AD afflicts more than 5 million individuals in the United States and 24 million people worldwide, with this number projected to double in 20 years.

Pathologically, AD is characterized by the temporal and spatial progression of amyloid plaques arising from extracellular deposition of the fibrillogenic amyloid-beta ( $A\beta$ ) peptide and other proteins, and intracellular neurofibrillary tangles (NT) due to the hyperphosphorylation of the microtubules-stabilizing protein Tau.

At the cellular level, AD is further associated with progressive dismantling of synapses, neuronal circuits and networks, and eventual neuronal loss within brain regions underlying cognition and memory formation (DeKosky and Sheff, 1990). Loss of synapses is considered the best correlate of cognitive decline in AD, rather than plaques or tangles.

### 1.1.1 $A\beta$ Peptide And Amyloid Cascade Hypothesis

More than 30 years ago, amyloid peptides were recognized by Glenner (Glenner and Wong, 1984) as a major component of the amorphous plaque-like deposits in the damaged brains of AD patients. Since then, a lot of evidence has demonstrated that  $A\beta$  peptide has potential neurotoxic properties (Yankner

*et al.*, 1989). Four other key discoveries have pointed out on the role of this peptide in the pathogenesis of disease. First, A $\beta$  peptide is part of a large type I membrane protein, the Amyloid Precursor Protein (APP), which is encoded by the *APP* gene on chromosome 21. Second, the *APP* gene is mutated in a significant fraction of familial AD cases. Third, individuals with Down's syndrome, who have three copies of chromosome 21 and hence three copies of *APP* gene, develop clinical and pathological signs of early onset Alzheimer's. And fourth, mutations of presenil-1 (*PSEN1*) and presenil-2 (*PSEN2*) genes, which encode for the catalytic subunit of the  $\gamma$ -secretase activity that liberates the A $\beta$  peptide from the C-terminus of APP, can behave as dominant familial AD genes.

These findings led to the elaboration of a theory of AD known as **amyloid cascade hypothesis** (Hardy and Selkoe, 2002; Citron, 2004), which best describes the pathogenic events causing Alzheimer neuronal death and leading ultimately to irreversible dementia. Indeed, this hypothesis postulates that in familial AD mutations in either APP or one of the PSEN genes lead to the brain accumulation of a 42-amino acid form of the amyloid peptide that has a tendency to form aggregates. Amyloid aggregates form first small oligomers and finally plaques. The amyloid cascade hypothesis proposes that these A $\beta$  aggregates leads in turn to a series of downstream events such as plaque deposition, tau hyperphosphorylation, inflammation, loss of synaptic structure and function, and death of susceptible neurons (Glennner and Wong, 1984; Tanzi and Bertram, 2005; Walsh and Selkoe, 2004). The hypothesis also proposes that sporadic AD develops when natural history of an individual accelerates a normal age-dependent process of A $\beta$  accumulation. At some

point, sufficient A $\beta$  become deposited that the amyloid cascade is triggered. Subsequently, the sporadic disease follows the same pathway to dementia as the familial form. Therefore, both in familial and sporadic AD the amyloid cascade hypothesis claims that is the excessive accumulation of pathogenic A $\beta$  assemblies in the brain to play a causal role in AD. Indeed, under normal conditions, A $\beta$  is present in a soluble form throughout life, but in Alzheimer's Disease pathogenesis, A $\beta$  aggregates into higher-order species such as soluble oligomers and insoluble amyloid plaques in a concentration-dependent manner.

In strong support of the pathogenic role of A $\beta$ , neuronal expression of human APP(hAPP) and A $\beta$  in transgenic mice elicits several AD-like abnormalities, including amyloid plaques, neuritic dystrophy, aberrant sprouting of axon terminals, functional and structural synaptic deficits, impairments in learning and memory, and other behavioral alterations (Chin *et al.*, 2004, 2005; Games *et al.*, 1995; Götz *et al.*, 2004; Kobayashi and Chen, 2005; Palop *et al.*, 2003, 2005).

### **1.1.2 APP processing and A $\beta$ generation**

The proteolytic processing pathways leading to the formation of A $\beta$  from the amyloid precursor protein (APP) have been well characterized in a number of cell lines (Selkoe, 2000). APP is a type I transmembrane protein. It is synthesized in the endoplasmic reticulum (ER) and then transported through the Golgi apparatus to the trans-Golgi network (TGN), where is found the highest concentration of APP in neuron at steady-state. From the TGN, APP can be transported in TGN-derived secretory vesicles to the cell surface, where

it is either cleaved by  $\alpha$ -secretase to produce a soluble molecule, sAPP $\alpha$ , or re-internalized via an endosomal/lysosomal degradation pathway.

At least three enzymes are responsible for the processing of APP and have been called  $\alpha$ -,  $\beta$ - and  $\gamma$ -secretases. The processing pathway by  $\alpha$ -secretase, called **non-amyloidogenic**, cleaves plasma membrane APP within the A $\beta$  domain in the C-terminal portion of the sequence of this peptide, producing soluble APP $\alpha$ , which has neurotrophic and neuroprotective effects. The processing pathway by  $\beta$ - and  $\gamma$ -secretases, called **amyloidogenic**, cleaves APP in the N- and C-terminal portions of the A $\beta$  region, respectively, producing A $\beta$  peptide.

Cleavage of APP by  $\alpha$ -secretase precludes A $\beta$  generation as the cleavage site is within the A $\beta$  domain and releases a large soluble ectodomain of APP called sAPP $\alpha$ . APP molecules that fail to be cleaved by  $\alpha$ -secretase on the membrane surface can be internalized into endocytic compartments and subsequently cleaved by  $\beta$ -secretase (BACE) and  $\gamma$ -secretase to generate A $\beta$ . After  $\alpha$ - and  $\beta$ -cleavage, the carboxyl terminal fragments (CTFs) of APP, known as  $\alpha$ CTF and  $\beta$ CTF, respectively, remain membrane associated.  $\alpha$ CTF and  $\beta$ CTF will be further cleaved by  $\gamma$ -secretase generating p83 and A $\beta$ , respectively. The p83 fragment is rapidly degraded and widely believed to possess no important function.  $\gamma$ -cleavage can yield both A $\beta$ 40, the majority species, and A $\beta$ 42, the more amyloidogenic species, as well as release intracellular domain of APP (AICD).

Although the majority of A $\beta$  is secreted out of the cell, A $\beta$  can be generated in several subcellular compartment within the cell, such as ER,

Golgi/TGN and endosome/lysosome. Then, A $\beta$  peptides generated in the Golgi and in recycling compartments can be secreted into the extracellular space (Greenfield *et al.* 1999). In addition, extracellular A $\beta$  can be internalized by the cell for degradation. The intracellular existence of A $\beta$  implies that it may accumulate within neurons and contribute to disease pathogenesis. The majority of secreted A $\beta$  peptides are 40 amino acids in length (A $\beta$ 40), although the smaller fraction (10%) of longer, 42 amino acid species (A $\beta$ 42) have received greater attention due to the propensity of these peptides and other derivatives of the amyloid precursor protein to nucleate and drive production of amyloid fibrils (Jarrett *et al.*, 1993). Studies done on familial AD mutations show increases in the ratio of A $\beta$ 42/A $\beta$ 40, suggesting that elevated levels of A $\beta$ 42 relative to A $\beta$ 40 is critical for AD pathogenesis, probably providing the core for A $\beta$  assembly into oligomers, fibrils and amyloidogenic plaques.

$\alpha$ -secretase is a membrane-bound endoprotease which cleaves APP primarily at the plasma membrane. In particular,  $\alpha$ -secretase is a zinc metalloproteinase. Its activity is constitutive, but it can also be regulated by various factors. Several members of the ADAM family possess  $\alpha$ -secretase-like activity and three of them have been suggested as the  $\alpha$ -secretase: ADAM9, ADAM10 and ADAM17. Like APP, they are also type-I transmembrane proteins. ADAM17 likely affects regulated, but not constitutive,  $\alpha$ -cleavage of APP in various cell lines; in contrast, ADAM10 is the constitutive  $\alpha$ -secretase that is active at the cell surface, as demonstrated by the inhibitor effect of ADAM10 dominant-negative form and *RNAi* of ADAM10 on the endogenous  $\alpha$ -cleavage activity in several cell lines. ADAM9 also shows  $\alpha$ -secretase activity, but it is involved only in the regulated  $\alpha$ -cleavage as ADAM17.

The major  $\beta$ -secretase is BACE1, that is a membrane-bound aspartyl protease. Several studies have confirmed that BACE-1 is the  $\beta$ -secretase involved in APP metabolism; and BACE1 activity is thought to be the rate-limiting factor in A $\beta$  generation from APP. BACE-1 requires an acidic environment for optimal activity; in fact, it is mainly found in the early Golgi, late Golgi/early endosomes, and endosomes that provide an acidic environment. In addition, BACE1 can be found at the cell surface. Several studies have found that BACE1 protein and activity levels are elevated in the regions of the brain affected by AD.

A lot of biochemical evidence has shown that  $\gamma$ -secretase activity resides in a high molecular weight complex consisting of at least four components: presenilin (PS, PS1 or PS2), Nicastrin, anterior pharynx-defective-1 (APH-1), and Presenil enhancer-2 (PEN-2). In mammals, there are two presenilin homologs, PS1 and PS2. Mutations in these two genes, particularly PS1, are causative in the majority of familial AD cases. PSs are multi-transmembrane proteins with an unclear number of transmembrane domains; they possess two highly conserved aspartate residues indispensable for  $\gamma$ -secretase activity and they are the crucial catalytic components of  $\gamma$ -secretase, as confirmed by *in vitro* assays. (Fig. 1)

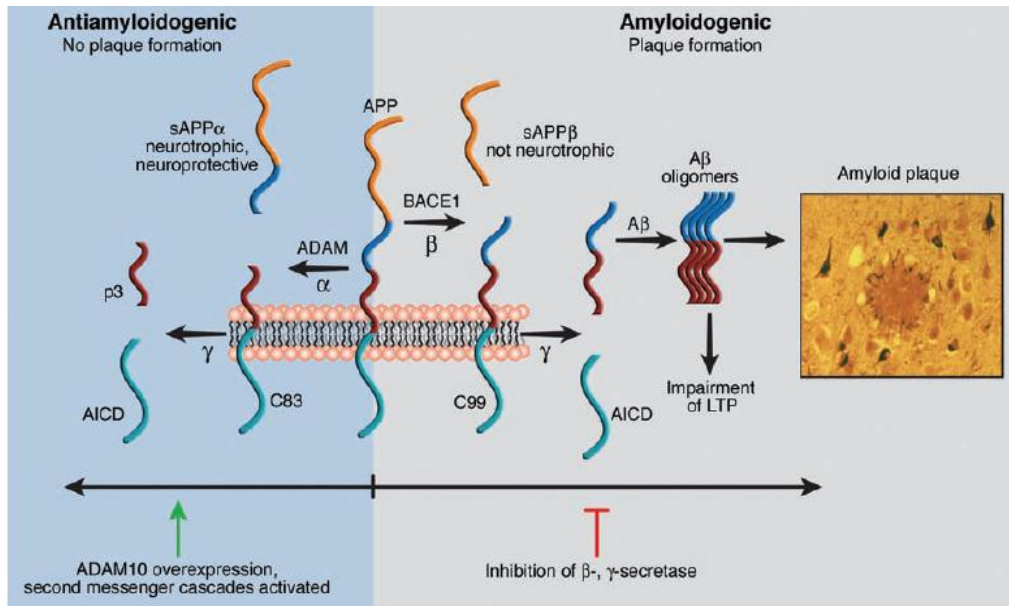


Figure 1. APP processing: non-amyloidogenic and amyloidogenic pathways.

### 1.1.3 A $\beta$ Affects Neuronal Excitability

Excessive accumulation of A $\beta$  is thought to be a causal factor in producing cognitive deficits, but the mechanisms by which A $\beta$  accumulation leads to this deficits is still unclear. Mounting evidence suggests that epileptiform activity may play an important role in the development of AD-related cognitive deficits. In fact, while seizures were previously thought to be secondary to disease progression, aberrant activity and/or seizures may directly contribute to cognitive deficits early in disease progression inducing hippocampal dysfunction and memory deficits.

AD is associated with a 5- to 10-fold increase in seizure incidence (Amatniek *et al.*, 2006; Hauser *et al.*, 1986; Hesdorffer *et al.*, 1996; Lozsadi and Larner, 2006; Mendez and Lim, 2003), and transgenic mouse models of AD exhibit brain-wide aberrant neuronal and epileptiform activity (Hsiao *et al.*, 1995; LaFerla *et al.*, 1995; Moechars *et al.*, 1999; Lalonde *et al.*, 2005; Palop *et*

*al.*, 2007; Minkeviciene *et al.*, 2009; Vogt *et al.*, 2009; Harris *et al.*, 2010; Roberson *et al.*, 2011; Sanchez *et al.*, 2012). Interestingly, the risk of epileptic activity is particularly high in AD patients with early-onset dementia and during the earlier stages of the disease, reaching an 87-fold increase in seizure incidence compared with an age-matched reference population (Amatniek *et al.*, 2006; Mendez *et al.*, 1994). The incidence of epileptic activity is also increased in sporadic AD (Amatniek *et al.*, 2006) but is particularly high in pedigrees with early-onset autosomal dominant AD (Cabrejo *et al.*, 2006; Larner and Doran, 2006; Palop and Mucke, 2009; Snider *et al.*, 2005). Epileptiform activity has been associated with transient episodes of amnesic wandering and disorientation in AD (Rabinowicz *et al.*, 2000).

Recent studies indicate that A $\beta$  peptide can contribute to AD cognitive decline inducing neuronal hyperexcitation and aberrant network activity. Neuronal circuits are smaller assemblies of interconnected neurons within a specific brain region and neuronal networks are larger assemblies of interconnected circuits involving different brain regions. Several recent reports in Alzheimer's disease-related mouse models suggest that pathologically elevated A $\beta$  destabilizes neuronal activity at the circuit and network levels. In particular, high A $\beta$  could induce aberrant excitatory network activity and compensatory inhibitory responses involving learning and memory circuits, leading to cognitive dysfunction. In fact, Palop *et al.*, 2007 report that transgenic mouse models of AD overexpressing A $\beta$  peptide exhibit altered neuronal activity, spontaneous seizures and epileptiform discharges within the entorhinal-hippocampal circuitry. They propose that the epileptiform activity together with homeostatic responses to this epileptiform activity may contribute

to dysfunction of the circuitry that underlies memory formation because blocking A $\beta$ -induced epileptiform discharges can meliorate cognitive decline and behavior dysfunction in these AD mouse models.

Soluble, rather than amyloid plaques, correlates well with the severity of cognitive decline and leads to malfunction of neurons. In fact, the hippocampal region of AD mouse model has an increased proportion of hyperactive neurons prior to the formation of A $\beta$  plaques (Cleary JP, *et al.* 2005). Moreover, application of A $\beta$ <sub>1-42</sub> to the extracellular medium induces CA1 neuron hyperactivity in wild type mice (Minkeviciene *et al.* 2009). These findings demonstrate that soluble A $\beta$  is involved in the neuronal hyperexcitation, aberrant network activity and cognitive impairment in AD.

However, the molecular mechanisms by which A $\beta$  can contribute to the destabilization of neuronal networks are poorly understood.

#### **1.1.4 Mouse Models Of Alzheimer's Disease**

Various transgenic models of Alzheimer disease (AD) were generated in the last decade in order to advance our understanding of *in vivo* responses to amyloid insult and the mechanism by which genetic alterations may cause AD. Indeed more features of the human disease are represented in these mice. Moreover, the mice are now being used to test therapeutic agents that may have utility in patients with AD.

The discovery of genes for familial forms of AD has allowed to create transgenic models that reproduce many critical aspects of the disease. Initially, before the discovery of FAD mutations, attempts were made to overexpress wild-type APP in transgenic mice. However, none of these efforts produced

anything that resembled an A $\beta$  plaque or any other recognizable AD-type pathology. After the discovery of FAD mutations in APP, a number of groups turned their attention to making AD models based on the overexpression of transgenes containing FAD mutations using a variety of promoters.

Mutations in APP linked to FAD include Dutch (E693Q), London (V717I), Indiana (V717F), Swedish (K670N/M671L), Florida (I716V), Iowa (D694N), and Arctic (E693G) mutations. To date, more than 160 mutations in PS1 linked to FAD have been discovered. Mutations in a PS2 gene were soon linked to FAD as well. Most of FAD mutations cause aberrant APP processing toward the longer, more amyloidogenic A $\beta$ <sub>1-42</sub> species. The Swedish mutation, which is located just outside the N-terminus of the A $\beta$  domain of APP, favors  $\beta$ -secretase cleavage *in vitro* and is associated with an increased level and deposition of A $\beta$ <sub>1-42</sub> in AD brain.

Report of the first transgenic mouse to develop a robust AD-related phenotype was published in 1995 (Games D *et al.*, 1995). This line, named PDAPP, overexpresses a human APP transgene containing the Indiana mutation (V717F). After that, in 1996, Karen Hsiao and colleagues created a second mouse line, termed Tg2576, which overexpresses a human APP transgene containing the Swedish mutation (K670N/ M671L). Subsequently, many other transgenic lines were developed with approaches similar to those used to develop PDAPP and Tg2576 mice, characterized by overexpression of one or more human APP mutations alone or combined with mutations of PS1 gene (**Table 1**).

Table 1 - Neuropathological features of the main transgenic mouse models of Alzheimer disease.

Mouse model	Gene (mutation)	Intraneuronal A $\beta$	Parenchymal A $\beta$ plaques	Hyperphosphorylated Tau	Neurofibrillary tangles	Neuronal loss	Synaptic loss	CAA	Primary reference
PDAPP	APP (V717F)	-	Yes	Yes	No	No	Yes	-	Games et al. 1995
Tg2576	APP (K670N/M671L)	Yes	Yes	-	-	No	No	-	Hsiao et al. 1996
TgCRND8	APP (K670N/M671L, V717F)	-	Yes	-	No	No	-	-	Chishti et al. 2001
APP/PS1	APP (K670N/M671L), PS1 (M146L)	-	Yes	-	-	-	-	-	Holcomb et al. 1998
APP23	APP (K670N/M671L)	-	Yes	Yes	No	Little	Yes	Yes	Sturchler-Pierrat et al. 1997
Tg-SwDI	APP (E693Q, D694N)	-	Yes	-	-	-	-	Yes	Davis et al. 2004
APPDutch	APP (E693Q)	-	Little	-	-	-	-	Yes	Herzig et al. 2004
APPDutch/PS1	APP (E693Q), PS1 (G384A)	-	Yes	-	-	-	-	Little	Herzig et al. 2004
hAPP-Arc	APP (E693G, K670N/M671L, V717F)	-	Yes	-	-	-	-	Little	Cheng et al. 2004
Tg-ArcSwe	APP (E693G, K670N/M671L)	Yes	Yes	-	-	-	-	Yes	Lord et al. 2006
APP <sub>sw</sub>	APP (E693G)	-	Yes	-	-	-	-	Yes	Knobloch et al. 2007
TAPP	APP (K670N/M671L), Tau (P301L)	-	Yes	-	Yes	-	-	-	Rönnbäck et al. 2011
3xTg-AD	APP (K670N/M671L), Tau (P301L), PS1 (M146V)	Yes	Yes	Yes	Yes	-	No	-	Lewis et al. 2001
APP <sub>sw</sub> /PS1	APP (K670N/M671L, V717I), PS1 (M146L)	Yes	Yes	-	-	Yes	Yes	-	Oddo et al. 2003
APP/PS1KI	APP (K670N/M671L, V717I), PS1 (M233T/L235P)	Yes	Yes	-	-	Yes	Yes	-	Wirths et al. 2002
5xFAD	APP (K670N/M671L, I716V, V717I), PS1 (M146L/L286V)	Yes	Yes	-	-	Yes	Yes	-	Casas et al. 2004
						Yes	Yes	-	Oakley et al. 2006

CAA = cerebral amyloid angiopathy; Dash (-) = not reported.

Table 1: mouse models of Alzheimer's Disease (Schaeffer EL *et al.* 2011).

**Tg2576** have been the most widely studied AD transgenic model because exhibits age-dependent increase of A $\beta$ 1-40 and A $\beta$ 1-42 levels and A $\beta$  deposition, resulting in senile plaques similar to those found in AD. A $\beta$  plaques were first clearly seen by 11-13 months, eventually becoming widespread in cortical and limbic structures. A $\beta$  deposits were associated with prominent gliosis and neuritic dystrophy, without overt neuronal loss in the hippocampal CA1 field or apparent synapse loss in the hippocampal dentate gyrus. Tg2576 mice exhibited deficits in synaptic plasticity in the hippocampal CA1 field and dentate gyrus, decreased dendritic spine density in the dentate gyrus, and impaired spatial memory and contextual fear conditioning months before significant A $\beta$  deposition, which was detectable at 18 months of age. A spine density decrease was detected as early as 4 months of age, and synaptic dysfunction and memory impairment were observed by 5 months. Moreover, an increase in the ratio of soluble A $\beta$ 1-42/A $\beta$ 1-40 was first observed at these early ages (4-5 months). Tg2576 mice also showed increased intraneuronal A $\beta$ 1-42

accumulation with aging, and this accumulation was associated with abnormal synaptic morphology before A $\beta$  plaque pathology.

## **1.2 Intrinsic membrane properties of Neurons and Voltage Gated Na<sup>+</sup> Channels**

Neurons are highly polarized cells with multiple distinct membrane domains by which they can integrate excitatory and inhibitory synaptic potentials into an output of action potentials. Both, the input/output relation of a neuron and the waveform of an action potential depend on the intrinsic properties of the neuron. These are determined by the neuron's endowment of voltage- and ion-gated ion channels. In neurons, action potentials (APs) are generated at the axonal initial segment (AIS), and their saltatory conduction occurs via the nodes of Ranvier in myelinated axons.

These processes require a precise distribution of voltage-gated sodium (Nav) channels, which accumulate at high density in these two highly specialized axonal sub-domains and upon depolarization permit the influx of Na<sup>+</sup> ions responsible of the rapid upstroke of action potentials.

### **1.2.1 Voltage Gated Na<sup>+</sup> Channels Structure**

Nav channels are integral membrane proteins that are predominantly expressed in excitable cells such as muscle cells and neurons. Expression of voltage gated Na<sup>+</sup> channels was also reported in other cell types such as glial cells ([Chiu *et al.* , 1984) and endothelial cells (Gordienko & Tsukahara, 1994).

Mammalian voltage-gated Na<sup>+</sup> channels (Nav) complex is typically a heterodimeric or heterotrimeric structure with a single pore-forming 260 kDa  $\alpha$

subunit associated with one or two accessory  $\beta$ -subunits (33-36 kDa). The  $\alpha$ -subunit contains the  $\text{Na}^+$  selective pore, the voltage sensor, and the channels activation and inactivation gate. It has been shown that  $\alpha$ -subunits alone are sufficient to give rise to a voltage sensitive  $\text{Na}^+$  current when expressed in various expression systems (Catterall, 2000). Association of  $\beta$ -subunits modulates  $\text{Na}^+$  channel kinetics and voltage dependence of activation and inactivation, and regulate the surface density of Nav1 (Isom, 2001, Isom, 2002, Qu *et al.* , 2001). (Fig. 2)

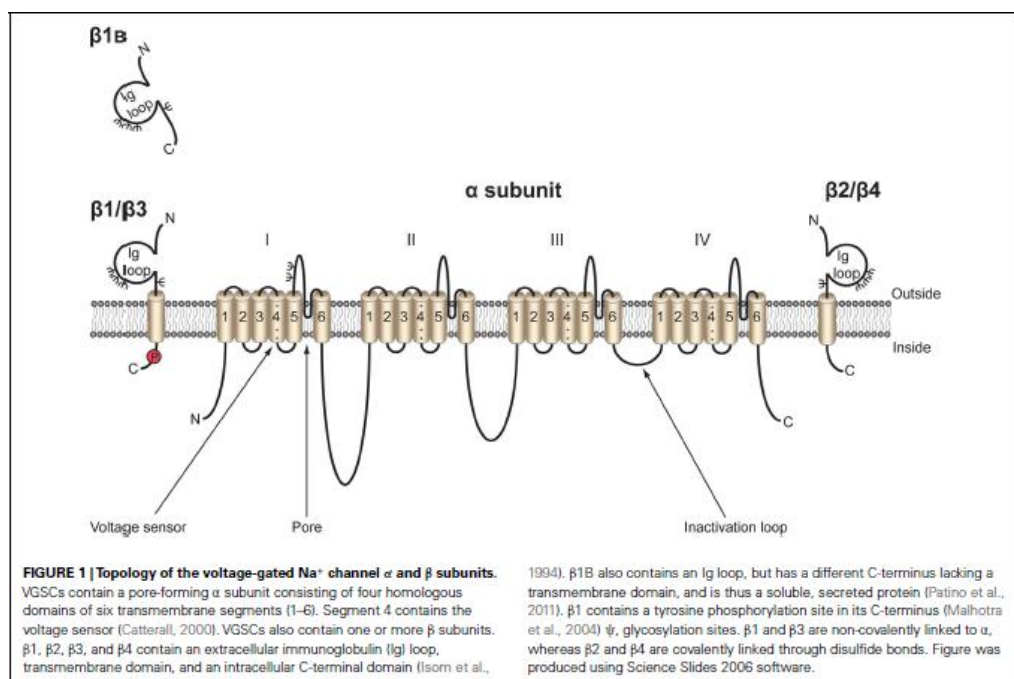


**Figure 2. Topology of voltage-gated  $\text{Na}^+$  channel  $\alpha$  and  $\beta$  subunits (Brackenbury and Isom, 2011).**

A functional voltage gated  $\text{Na}^+$  channel  $\alpha$ -subunit contains four homologous domains (DI-DIV), each of them consisting of six transmembrane  $\alpha$ -helices (S1-S6). Within each domain the S4 segment forms a part of the  $\text{Na}^+$  channel's voltage sensor, which undergoes a conformational change upon depolarization whose movement within the membrane induces in pore opening (Terlau and

Stühmer, 1998). The transmembrane  $\alpha$ -helices S5 and S6 form the inner part of the ion channel pore, whereas the linker region between these two segments reaches into the outer leaflet of the membrane's lipid bilayer and forms the outer part of the ion channel pore. The intracellular loop between domain III and IV serves as an inactivation gate that blocks the open channel upon prolonged depolarization (Stühmer *et al.* , 1989, Catterall *et al.* , 2005).

The linkers between the four domains vary in length and have important functions in channel modulation, inactivation, and drug binding as well as the binding sites for the toxins tetrodotoxin (TTX) or  $\mu$ -conotoxin. Interactions with other proteins also take place within these linker domains. Such interactions are either intracellularly, as the binding to cytoskeleton associated proteins or extracellularly, as binding to  $\text{Na}^+$  channel  $\beta$ -subunits.

$\beta$ -Subunits of  $\text{Na}_v$  belong to the immunoglobulin superfamily of cell adhesion molecules and associate with  $\alpha$ -subunits in two ways: covalently in the case of  $\text{Na}_v\beta 2$  and  $\text{Na}_v\beta 4$  subunits through a disulfide bridge in the extracellular domain and non-covalently for  $\text{Na}_v\beta 1$  and  $\text{Na}_v\beta 3$  subunits (Patino and Isom, 2010).  $\text{Na}_v$   $\beta$ -subunit expression is widespread both in excitable and non-excitable tissues (Patino and Isom, 2010).

The  $\text{Na}_v\beta$  subunits share a similar topology. Structurally, they consist of a single transmembrane domain and larger extracellular than intracellular domains.  $\text{Na}_v\beta$ -subunits are multifunctional, acting to modify channel gating, regulate channel expression in the plasma membrane; independent of their role in sodium channel association, they serve as cell adhesion molecules in interactions with the extracellular matrix and as well as the cytoskeleton and intracellular signaling molecules (Isom, 2002; Brackenbury and Isom, 2011); in

fact,  $\beta$ -subunit soluble ectodomain and membrane bound C-terminal fragment obtained by their enzymatic cleavage are implicated in the regulation of cell–cell contact and neurite outgrowth (Wong *et al.*, 2005).

### **1.2.2 Sodium Channel Classification and Nomenclature**

The sodium channels are members of the superfamily of ion channels that includes voltage-gated potassium and calcium channels (Yu and Catterall, 2004); however, unlike the different classes of potassium and calcium channels, the functional properties of the known sodium channels are relatively similar.

In the standardized nomenclature system, the name of an individual channel consists of the chemical symbol of the principal permeating ion ( $\text{Na}^+$ ) with the principal physiological regulator (voltage) indicated as a subscript ( $\text{Na}_V$ ). The number following the subscript indicates the gene subfamily (currently only  $\text{Na}_V1$ ), and the number following the full point identifies the specific channel isoform (e.g.,  $\text{Na}_V1.1$ ). This last number has been assigned according to the approximate order in which each gene was identified. Splice variants of each family member are identified by lowercase letters following the numbers (e.g.,  $\text{Na}_V1.1a$ ). In mammals, there are nine different genes, *Scn1a* to *Scn11a*, encoding the nine monomeric  $\alpha$ -subunits of voltage gated  $\text{Na}^+$  channels,  $\text{Na}_V1.1$  to  $\text{Na}_V1.9$  which share about 80% of their sequence (Catterall *et al.*, 2005) (Fig. 3).

Type	Gene symbol	Chromosomal location	Primary tissues
Na <sub>v</sub> 1.1	SCN1A	Mouse 2 Human 2q24	CNS neurons
Na <sub>v</sub> 1.2	SCN2A	Mouse 2 Human 2q23–24	CNS neurons
Na <sub>v</sub> 1.3	SCN3A	Mouse 2 Human 2q24	CNS neurons
Na <sub>v</sub> 1.4	SCN4A	Mouse 11 Human 17q23–25	SkM
Na <sub>v</sub> 1.5	SCN5A	Mouse 9 Human 3p21	Uninnervated SkM, heart
Na <sub>v</sub> 1.6	SCN8A	Mouse 15 Human 12q13	CNS neurons
Na <sub>v</sub> 1.7	SCN9A	Mouse 2 Human 2q24	PNS neurons
Na <sub>v</sub> 1.8	SCN10A	Mouse 9 Human 3p22–24	DRG neurons
Na <sub>v</sub> 1.9	SCN11A	Mouse 9 Human 3p21–24	DRG neurons
Na <sub>x</sub>	SCN7A SCN6A	Mouse 2 Human 2q21–23	uterus, astrocytes, hypothalamus

**Figure 3. Mammalian Na<sub>v</sub>  $\alpha$  subunits (*J Physiol* 590.11 (2012))**

Five sodium channel  $\beta$  subunits have been described so far: Na<sub>v</sub> $\beta$ 1, Na<sub>v</sub> $\beta$ 2, Na<sub>v</sub> $\beta$ 3, and Na<sub>v</sub> $\beta$ 4, encoded by four different genes (SCN1B–SCN4B).

Protein	Gene Symbol (Human)	Tissue Location
$\beta$ 1	SCN1B	Heart, skeletal muscle, CNS, glia, PNS
$\beta$ 1A ( $\beta$ 1B)	SCN1B	Heart, skeletal muscle, adrenal gland, PNS
$\beta$ 2	SCN2B	CNS, PNS, heart, glia
$\beta$ 3	SCN3B	CNS, adrenal gland, kidney, PNS
$\beta$ 4	SCN4B	Heart, skeletal muscle, CNS, PNS

Abbreviations: VGSC = voltage-gated Na<sup>+</sup> channel; PNS = peripheral nervous system; DRG = dorsal root ganglia.

**Figure 4. Classification and distribution of Na<sub>v</sub>  $\beta$  subunits (Branckebury *et al.*, 2008)**

### 1.2.3 Voltage Gated Na<sup>+</sup> Channels Functional Expression

The voltage-gated Na<sup>+</sup> channels Nav1.1–1.9 are all expressed in excitable tissues. With the exception of Nav1.4, that is expressed only in the skeletal muscle, all Nav1 subunits are expressed in the nervous system. Nav1.1, 1.2, 1.3, and 1.6 are most predominant subtypes in CNS. Nav1.5 is the major cardiac sodium channel, whereas Nav1.7, 1.8, and 1.9 are important players in nociceptive signaling transduction owing to their presence in peripheral primary sensory afferents. (Catterall *et al.* , 2005).

Navβ1, Navβ2 and Navβ4 are the main Navβ subunits expressed in the mammalian brain.

Both the expression of the four predominant Nav1 subtypes and the four β subunits are developmentally and spatially regulated in the CNS. Nav1.3 channels are primarily expressed in embryonic and neonatal rodent brain, whereas it is poorly expressed in the rodent adult brain. In contrast, Nav1.3 expression remains high in adult human brain (Chen *et al.*, 2000;Whitaker *et al.*,2001). Nav1.1, Nav1.2, and Nav1.6 display developmentally regulated expression patterns in specialized neuronal subcellular domains. In fact, Nav1.1 is localized primarily in the soma of CNS neurons; it is also found in the dendrites, but it is dominant at the AIS of GABAergic neurons, retinal ganglion cells and in spinal cord motoneurons and nodes of Ranvier. Nav1.6 and Nav1.2 are principally associated with AIS of myelinated and unmyelinated axons, respectively, with Nav1.2 expressed first during development, then being gradually replaced by Nav1.6 concomitantly with myelination (Kaplan *et al.*, 2001). Although greatly diminished, the expression of Nav1.2 might persist in the AIS of adult neurons and is maintained in populations of unmyelinated

axons (Jarnot and Corbett, 1995; Boiko *et al.*, 2003 ). The two isoforms coexist in the AIS of L5 pyramidal neurons with a proximal distribution of Nav1.2 and a distal distribution of Nav1.6. Sodium channels in the distal part of the AIS display the lowest threshold, suggesting that this polarized distribution could explain the unique properties of the AIS, including action potential initiation (principally mediated by Nav1.6) and backpropagation (largely supported by Nav1.2). A similar conclusion is drawn in CA1 pyramidal neurons where Nav1.6 sodium channels play a critical role for spike initiation. Nav1.6 is also concentrated nodes of Ranvier in myelinated axons (Schaller and Caldwell, 2000; Boiko *et al.*, 2001; Boiko *et al.*, 2003; Van Wart and Matthews, 2006; Van Wart *et al.*, 2007; Lorincz and Nusser, 2008, 2010), and is found at lower abundance in neuronal soma and proximal dendrites (Krzemien *et al.*, 2000; Lorincz and Nusser, 2010).

Little information is available on  $\beta$  subunit localization at the cellular level, although Nav $\beta$ 2 may be concentrated at the nodes of Ranvier and Nav $\beta$ 1 has been detected at the AIS in cerebellar GCs. Sodium channels in the adult central nervous system contain Nav $\beta$ 1 through Nav $\beta$ 4 subunits (Isom, 2001).

#### 1.2.4 Types of Nav currents

The voltage gated Na<sup>+</sup> channels give rise to a prominent transient Na<sup>+</sup> current ( $I_{NaT}$ ) and to two smaller Na<sup>+</sup> currents, namely the persistent Na<sup>+</sup> current ( $I_{NaP}$ ) (French *et al.* , 1990) and the resurgent Na<sup>+</sup> current ( $I_{NaR}$ ) (Raman & Bean, 1997).

The **transient Na<sup>+</sup> current** initiates and mediates the fast rising phase of the action potential. At resting membrane potentials, Nav channels are closed,

requiring depolarization to be activated. A small depolarization of the neuronal membrane potential in response to sensory input or receptor input depolarizes the neuronal membrane potential to the threshold for  $\text{Na}_v$  activation ( $\sim -50$  mV).  $\text{Na}_v$ s activate rapidly ( $\sim 1$  ms to peak) allowing the influx of sodium in an inward direction dictated by the electrochemical gradient and depolarizing the membrane potential further, forming the upstroke of the action potential.  $\text{Na}_v$  channels close within 1–2ms of opening, a process called fast inactivation that changes the channels to a non-conducting state contributing to the downstroke of the action potential. Channel inactivation persists through-out the depolarizing pulse, thus underlying the action potential refractory period. In addition to fast inactivation,  $\text{Na}^+$  channels also undergo slow inactivation, which does not primarily depend on the fast inactivation gate. Following hyperpolarization of the membrane potential, the channel recovers from inactivation by returning to the closed, resting state and is re-primed and available again for activation. Recovery from fast as well as slow inactivation is time dependent and leads to a refractory period during which depolarization fails to open the channel pore. Moreover, recovery from inactivation allows the channels to participate in the next action potential and it is required for repetitive firing of action potentials in neural circuits and for control of excitability in nerve and muscle cells.

All the kinetically fast transient channels ( $\text{Na}_v1.1$ – $1.7$ ) appear quite similar in functional properties, but in many neurons sodium channels sometimes generate much longer openings as a result of incomplete or defective fast inactivation of  $\text{Na}^+$  channels and a **persistent  $\text{Na}^+$  ( $I_{\text{NaP}}$ ) current** can be recorded (French *et al.* , 1990, Crill, 1996, Magistretti & Alon-so, 1999).

$I_{NaP}$  inactivates over a time period of tens of seconds and its amplitude is just a few per cent of that of the transient current at the same potentials, but is still functionally important. The hyperpolarized voltage dependence of activation of persistent sodium currents allows these channels to operate as amplifiers of subthreshold depolarization, because their activation kinetics are fast and they operate over a strategic subthreshold membrane potential range with low potassium channel activation.

In some neurons, sodium channels transiently open upon recovery from inactivation when the membrane potential is repolarized. This transient opening gives rise to a large inward tail current termed **resurgent current**  $I_{NaR}$  (Cannon and Bean, 2010), that may be caused by a temporary block of the channel by an open-state channel blocker that prevents entry of channel into the true inactive state. In fact, this blocker precludes the entry of the inactivation gate into the pore resulting in a temporarily inactive state that is easily reversed by minor hyperpolarization of the cell (Aman and Raman, 2010). The inactivation released upon repolarization is thought not to depend on the inactivation gate of the  $Na^+$  channel  $\alpha$ -subunit itself. One possible mechanism for resurgent current involves the blockade of the channel pore by the C-terminus of  $Na_v\beta_4$  subunit of sodium channels, serving as an additional inactivation gate (Chen *et al.*, 2008 and Aman *et al.*, 2009). This rapidly reversible form of inactivation allows neurons to fire rapidly and repetitively.

### **1.2.5 Molecular basis of $Na_v$ currents**

The molecular mechanism by which changes in membrane voltage confer a conformational change on voltage-gated ion channel proteins is

through the movement of modular voltage sensors contained within the S4 segment of domains I–IV (Alabi *et al.*, 2007). Transmembrane segment S4 of each domain contains 3-5 positively charged residues that are essential for the channel response to changes in membrane potential. In response to membrane depolarization, electrostatic interactions between positively charged residues and the depolarized cytoplasm force S4 towards the extracellular surface. This results in a conformational change in S5-S6 that opens the channel pore and allows sodium influx (Yarov-Yarovo Y *et al.*, 2012). S4 segment of domains IV is also implicated in the voltage-dependent coupling of activation to inactivation. In fact, outward movement of this segment is the signal to initiate fast inactivation of the sodium channel by closure of the intracellular inactivation gate (Catterall, 2000).

The short highly conserved intracellular loop connecting homologous domains III and IV of the sodium channel  $\alpha$  subunit serves as an inactivation gate. This loop moves into the pore region, binds to the intracellular pore of the channel to inactivate it, preventing any additional current flow. Mutagenesis studies of this region revealed that a hydrophobic triad of isoleucine, phenylalanine, and methionine (IFM) is critical for fast inactivation; moreover, among these three amino acids, phenylalanine residue (F1489) is fundamental for the inactivation because it forms a hydrophobic interaction with an inactivation gate receptor during inactivation (Catterall, 2000).

### **1.3 Na<sub>v</sub>1.6 Sodium Channel**

Voltage-gated sodium channel Na<sub>v</sub>1.6 is encoded by the *Scn8a* gene, located on distal chromosome 15 in mouse (Burgess *et al.*, 1995b) and on

chromosome 12q13.13 in human (Plummer *et al.*, 1998). *Scn8a* is a large gene, with 27 exons, and encodes a 1980 residue protein.

Nav1.6 is broadly expressed in the nervous system in a variety of cells including Purkinje cells, motor neurons, pyramidal and granule neurons, glial cells and Schwann cells and is enriched at the nodes of Ranvier (Caldwell *et al.*, 2000; Kearney *et al.*, 2002). Nav1.6 is concentrated at the axon initial segment and nodes of Ranvier in myelinated axons (Schaller and Caldwell, 2000; Boiko *et al.*, 2001; Boiko *et al.*, 2003; Van Wart and Matthews, 2006; Van Wart *et al.*, 2007; Lorincz and Nusser, 2008, 2010), and is also found at lower abundance in neuronal soma and dendrites (Krzemien *et al.*, 2000; Lorincz and Nusser, 2010).

### **1.3.1 Unique Biophysical Properties Of Nav1.6**

The electrophysiological properties of Nav1.6 have been characterized in cultured cells and in neurons from mouse. Cell culture studies allow Nav1.6 to be studied in isolation from other channels, which is important for understanding its specific electrophysiological properties. *In vivo* studies of Nav1.6 have focused on using null mouse mutants to remove this channel in the context of the entire neuron, and provide critical insight into the role of this channel in the complex regulation of neuronal firing.

The role of Nav1.6 in regulating neuronal excitability may be related to the following properties: its voltage dependence of activation, its subcellular localization at the axon initial segment (AIS), the site of initiation of action potentials., and its role in persistent and resurgent current. The highest density of the Nav1.6 subunit is present in the AISs of all major neuron types of the

neocortex, hippocampus, cerebellum. The Nav<sub>v</sub>1.6 is preferred over the other Nav<sub>v</sub>α-subunits in the AISs because its activation threshold is shifted to a more hyperpolarized potential (by ~15–25 mV) compared with that of Nav1.2 (Rush *et al.*, 2005) and Nav1.1 subunits (Spampanato *et al.*, 2001), ensuring lower threshold for AP generation. Moreover, Nav<sub>v</sub>1.6 shows a reduced use-dependent inactivation at frequencies >20 Hz respect Nav1.2 (Rush *et al.*, 2005) and Nav1.1 subunits (Spampanato *et al.*, 2001) show a robust (Rush *et al.*, 2005), which would allow high frequency firing of nerve cells. Indeed, cerebellar Purkinje cells from mice lacking the Nav1.6 subunit (Raman *et al.*, 1997) showed impaired ability to fire bursts of APs at high frequencies.

The persistent current generated by Nav1.6 is five-fold higher than that generated by Nav<sub>v</sub>1.2 (Smith *et al.*, 1998, Rush *et al.*, 2005, Chen *et al.*, 2008). The larger persistent sodium currents of Nav<sub>v</sub>1.6 channels maintain depolarization of membrane potential near threshold and thereby permit firing of additional action potentials. The magnitude of persistent current depends on the specific cell type (Rush *et al.*, 2005; Chen *et al.*, 2008), suggesting that this property can be modulated by other factors and not only exclusively attributed to this subunit [Ma *et al.*, 1997].

Resurgent current has been widely associated with the presence of Nav<sub>v</sub>1.6. Indeed, in *Scn8amed* neurons lacking Nav<sub>v</sub>1.6 the amplitude of  $I_{NaR}$  is reduced. The resurgent currents of Nav1.6 channels generate inward current after each action potential and permit rapid recovery from inactivation, thereby facilitating high frequency firing (Raman and Bean, 1997; Levin *et al.*, 2006).

Larger relative levels of persistent and resurgent current render membranes containing Nav<sub>v</sub>1.6 more excitable than membranes containing the

neuronal channels  $Na_V1.1$  and  $Na_V1.2$ . Persistent current is important for populations of neurons that undergo repetitive firing and it has been hypothesized that resurgent current contributes to increased excitability leading to spontaneous firing and multiphased action potentials.

### 1.3.2 Regulative Protein Interactions Of $Na_V1.6$

Voltage-gated sodium channels are components of large, multi-protein complexes that vary between neurons and at specific subcellular domains. These multiple binding partners regulate gating properties and subcellular localization (Dib-Hajj and Waxman, 2010) of  $Na_V$  channels. Several protein interaction sites have been mapped to the intracellular loops and C-terminus of the channels.

**Microtubule-associated protein Map1b.** Map1b is a cytoskeletal protein that binds microtubules and actin (Riederer, 2007) and contributes to trafficking of several channel and receptor proteins. O'Brien et al. 2012 demonstrated that  $Nav1.6$  is another neuronal protein that is trafficked along the microtubule network to the cell surface by interaction with the light chain of Map1b. Since microtubules extend along the full length of the axon, Map1b could play a role in localization of  $Nav1.6$  to both the AIS and the nodes of Ranvier. The residues 77-80 (VAVP motif) in the N-terminus of  $Na_V1.6$  are responsible of interaction with the light chain of Map1b. Interestingly, this interaction may be specific to  $Na_V1.6$  because the VAVP motif is not conserved in the other  $Na_V$  channels; in fact  $Na_V1.1$  and  $Na_V1.2$  bind Map1b at a reduced affinity compared to  $Na_V1.6$  due to the difference in residues of the binding site. Moreover, O'Brien *et al.*, 2012 demonstrated that the interaction with Map1b

increases Nav1.6 peak current density resulting in an increase in current density enhancing trafficking of Nav1.6 to the cell surface without a change in activation or fast-inactivation of the channel.

**Protein kinases.** PKA and PKC have only a small effect on Nav1.6 channel activity (Chen *et al.*, 2008); in fact, the reduction of its current is only 7% by PKC and 8% by PKA, despite multiple predicted PKA and PKC phosphorylation sites (Chen *et al.*, 2008).

Immunohistochemistry of hippocampal neurons demonstrated that the MAP kinase p38 co-localizes with Nav1.6 (Gasser *et al.*, 2010). This stress-activated kinase phosphorylates Nav<sub>v</sub>1.6 at serine 553 of the first intracellular loop (Wittmack *et al.*, 2005). This phosphorylation creates a PXpS/TP motif (residues 551-554) that facilitates binding of E3 ubiquitin ligases, Nav<sub>v</sub>1.6 internalization and proteasomal degradation (Sudol and Hunter, 2000; Zarrinpar and Lim, 2000; Gasser *et al.*, 2010) inducing Nav1.6 current amplitude reduction, as observed in the ND7/23 cell line (Wittmack *et al.*, 2005) and in hippocampal neurons (Gasser *et al.*, 2010) treated with p38 activator, Anisomycin. Moreover, no effect of p38 on sodium current was observed in *Scn8a* null (*med*) hippocampal neurons, suggesting that Nav<sub>v</sub>1.6 is the predominant sodium channel target of activated p38 (Gasser *et al.*, 2010).

**Ankyrin (Ank).** Ankyrins are adaptor proteins that attach membrane proteins to spectrin components of the cytoskeleton. In the higher vertebrates, three genes encoding for Ankyrins (Ankyrin-R, Ankyrin-B and Ankyrin-G) are been identified: ANK1, ANK2 and ANK3. Direct interaction between ankyrins and voltage-gated sodium channels is well documented (Srinivasan *et al.*, 1988; Davis *et al.*, 1996; Hill *et al.*, 2008). All vertebrate voltage-gated sodium

channels share a conserved ankyrin-binding motif (nine residues) in the second cytoplasmic loop (Nav1.6 residues 1089-1122) (Lemaillet *et al.*, 2003; Gasser *et al.*, 2012), that is necessary for binding to Ankyrin G. It has been recently demonstrated that AnkG binding is essential for targeting and localization of Nav1.6 to the AIS and nodes of Ranvier (Gasser *et al.*, 2012). Interestingly, mutations in conserved residues of the ankyrin-binding motif do not alter the electrophysiological properties of Nav1.6 (Gasser *et al.*, 2012).

**Voltage-gated sodium channel  $\beta$  subunits.** Nav $\beta$ 1 (36 kDa) and Nav  $\alpha$  subunits are bound in non-covalent manner. In particular, negatively charged residues of extracellular domain and intracellular portion of Nav $\beta$ 1 are involved in the functional interaction with  $\alpha$  subunit (McCormick *et al.*, 1998; Spampinato *et al.*, 2004). Biskup *et al.* 2004 demonstrated that Nav $\beta$ 1 and Nav  $\alpha$  subunit associate in the endoplasmic reticulum, after that they reach the plasma membrane as a complex; this association is fundamental for the correct delivery to the membrane and localization of Nav  $\alpha$  subunit in specific neuronal domains.

Interaction between Nav $\beta$ 1 and Nav1.6 is required for function of Nav1.6 at the distal AIS (Brackenbury *et al.*, 2010). In fact, Nav $\beta$ 1 mediate functional association with AIS protein scaffold. Studies of mice null for the  $\beta$ 1 subunit (*Scn1b*<sup>-/-</sup>) suggest that interaction between  $\beta$ 1 and Nav1.6 is required for wild-type expression levels of Nav1.6 at the distal AIS *in vitro* and *in vivo* (Brackenbury *et al.*, 2010). A higher proportion of Nav1.1 was observed at the AIS in cultured cerebellar granule neurons and cerebellar Purkinje neuron slices from *Scn1b*<sup>-/-</sup> mice (Brackenbury *et al.*, 2010). As a consequence of reduced Nav1.6 at the AIS, slightly reduced levels of resurgent current were

observed in cerebellar granule neuron slices (Brackenbury *et al.*, 2010). Thus, the interaction between  $\beta 1$  and  $\text{Na}_V1.6$  is important for localization and function of the channel.

Sodium channel activity mediate neurite extension during development; in particular, functional reciprocity of  $\text{Na}_V1.6$  and  $\text{Na}_V\beta 1$  is involved in this process. In fact, Brackenbury *et al.*, 2010 demonstrated that transfection of  $\text{Na}_V\beta 1$  subunits into a monolayer of Chinese Hamster Lung cells co-cultured with isolated mouse brain neurons positively affects neurite extension in wild type neurons. Transfection of  $\text{Na}_V \beta 1$  had no effect on *Scn8a* null neurons in this co-culture system, demonstrating that some sodium channel current-dependent neurite outgrowth is mediated by  $\text{Na}_V1.6$ .

$\text{Na}_V\beta 4$  associates covalently  $\text{Na}_V \alpha$  subunit by disulfide bridge; indeed, one of the five cysteine residue of extracellular domain is involved in this bound.

Interaction of  $\text{Na}_V1.6$  and  $\text{Na}_V\beta 4$  has been implicated in the generation of resurgent current (Grieco *et al.*, 2005; Aman *et al.*, 2009). In cultured cerebellar neurons, the  $\beta 4$  subunit is required for generation of resurgent current and contributes to persistent current and repetitive firing (Bant and Raman, 2010). Knockdown of  $\beta 4$  by siRNA in cultured cerebellar granule cells reduced resurgent current from ~9% of transient current in control cells to ~3.7% in treated cells.  $\beta 4$  knockdown resulted in a 7.7 mV hyperpolarizing shift in the voltage dependence of inactivation and a decrease in repetitive firing, changes that are predicted to reduce neuronal excitability. Most, but not all, subpopulations of neurons that have resurgent current express the  $\beta 4$  subunit

(Bant and Raman, 2010). However, full-length  $\beta 4$  is not sufficient to generate resurgent sodium current.

**Calmodulin.** The intracellular concentrations of  $\text{Ca}^{2+}$  effect gating properties of  $\text{Na}_V$  channels activating Calmodulin/ Calmodulin Kinase II complexes that bind IQ domain of  $\text{Na}_V$  C-terminus (Deschenes *et al.*, 2002; Maltsev *et al.*, 2008; Mori *et al.*, 2003).

Calmodulin (CaM) is a ubiquitous, small (16,7 kDa) calcium-binding protein that acts as a  $\text{Ca}^{2+}$  sensor translating changes in cytoplasmic  $\text{Ca}^{2+}$  into cellular responses by interacting with a diverse group of signaling molecules. Ion channels are prominent targets of CaM, for example L-type voltage-dependent  $\text{Ca}^{2+}$  channels, but also  $\text{Na}_V$  channels. All of the voltage-gated sodium channels contain an IQ motif in the C-terminus (Yu and Catterall, 2003; Feldkamp *et al.*, 2011) by which they can associate CaM.

The IQ motif of  $\text{Na}_V 1.6$  is localized between residues 1902–1912 of carboxyl terminus of the channel. The same motif binds apo-CaM, the  $\text{Ca}^{2+}$  deficient form of calmodulin, and  $\text{Ca}^{2+}$ -bound CaM (Bahler and Rhoads, 2002). Herzog *et al.*, 2003 demonstrated that CaM regulates the current density and the kinetics properties of  $\text{Na}_V 1.6$  currents in a calcium-dependent manner. Indeed, the authors suggest that binding of apo-CaM to  $\text{Na}_V 1.6$  accelerates its inactivation; addition of  $\text{Ca}^{2+}$  to the system, converting apo-CaM to CaM, slowed  $\text{Na}_V 1.6$  inactivation by ~50% increasing excitability.

**Nedd4.** Nedd4 or *Neuronal precursor cell-expressed developmentally downregulated 4* is a E3 ubiquitin ligase responsible of ubiquitination and degradation of protein containing WW domains with PY motif.  $\text{Na}_V$  channels are target of ubiquitination by Nedd4.  $\text{Na}_V 1.6$  contains two binding sites for

Nedd4, a PXY motif (residues 1943–1945) at the C-terminus, and the PXpS/pTP motif in the first cytoplasmic loop (residues 551–554) (Abriel *et al.*, 2000; Sudol and Hunter, 2000; Fotia *et al.*, 2004; Ingham *et al.*, 2004), both necessary for internalization and degradation of Nav1.6 (Gasser *et al.*, 2010).

### 1.3.3 Nav1.6 Role In Pathophysiological Conditions

Nav1.6 appears to be particularly important, because it is the principal channel at axonal sites where action potentials are generated. Juvenile lethality of Nav1.6 deficit at postnatal day 21 (P21) suggests that this channel is vital for impulse propagation later in life, when it substitutes Nav1.2.

Within the past year, de novo mutations of human SCN8A detected by exome sequencing have revealed a role for Nav1.6 in epilepsy and intellectual disability. Hypoactivity and hyperactivity of Nav1.6 are both pathogenic, but with different outcomes: haploinsufficiency is associated with impaired cognition (Trudeau *et al.*, 2006; McKinney *et al.*, 2008; Rauch *et al.*, 2012) while hyperactivity can result in epilepsy (Veeramah *et al.*, 2012).

*Scn8a* gene mutations causing Nav1.6 loss or disruption result in a variety of recessive neuromuscular phenotypes, including tremor, cerebellar ataxia, dystonia and paralysis, as naturally occurring *med* mutant Nav1.6 (*Scn8amed*) knockout mice (Meisler *et al.*, 2002, 2004). The tremor and ataxia result from the altered biophysical properties, in particular reduced persistent and resurgent current and diminished spontaneous simple spikes (Levin *et al.*, 2006; Harris *et al.*, 1992; Raman *et al.*, 1997). In addition, prefrontal cortex pyramidal cells and retinal ganglion cells of the homozygous *Scn8amed*

mutants also show reduced excitability (Maurice *et al.*, 2001; Van Wart, A. and Matthews, 2006).

Na<sub>v</sub>1.6 has diverse and complex roles in epilepsy. Abnormally high levels of persistent Na<sub>v</sub>1.6 current causes neuronal hyperexcitability and leads to epilepsy (Veeramah *et al.*, 2012). Gain of function mutations cause convulsive seizures, as shown in a patient with infantile epileptic encephalopathy (Veeramah *et al.*, 2012). Conversely, Na<sub>v</sub>1.6 loss of function mutations cause absence seizures and are protective against convulsive seizures (Martin *et al.*, 2007). These divergent effects between seizure types are presumably due to independent roles of Na<sub>v</sub>1.6 in separate epileptic networks.

#### **1.4 Voltage-Gated Sodium Channels And Alzheimer's Disease**

Forms of epilepsy are accompanied by cognitive impairment. Elevated incidence of epilepsy has been demonstrated in patients with Alzheimer's disease, as well in AD-related mouse models that have elevated levels of A $\beta$  exhibit altered neuronal activity and hyperexcitability. Many papers highlight that Na<sub>v</sub> channels can give a strong contribute to the hypersynchronicity of neuronal brain circuits in AD. In fact, altered expression and processing of voltage-gated sodium channels have been described in AD mouse model and patients. Verret *et al.*, 2012 identified alterations in Na<sub>v</sub>1.1 channel in human amyloid precursor protein (hAPP) transgenic mice and AD brains. In particular, they demonstrated a reduction of Na<sub>v</sub>1.1 levels in inhibitory Parvalbumin cells, which prominently express this Na<sub>v</sub> subunit. The authors correlated this reduction to A $\beta$ -induced aberrant network activity and cognitive decline

because restoring physiological levels of this channel in hAPP mice they are able to enhance inhibitory synaptic currents and decrease network hypersynchronization and memory deficits.

Corbett *et al.*, 2013 confirmed the involvement of  $\text{Na}_V1.1$  in AD aberrant neuronal activity; in fact, they proved that surface expression of this  $\text{Na}_V$  channel is reduced in inhibitory and excitatory cortical neurons of Tg2576 AD mice model and that  $\text{Na}_V\beta2$  is responsible of this reduction. Kim *et al.*, 2007 previously had demonstrated that intracellular domain (ICD) of  $\text{Na}_V\beta2$  is able to control the protein expression of  $\text{Na}_V1$  translocating to the nucleus and triggers expression of this  $\text{Na}_V\alpha$  subunit. Interestingly,  $\text{Na}_V\beta2$  ICD is produced by proteolytic cleavage of BACE1 and  $\gamma$ -secretase enzymes, like APP. When Kim *et al.*, 2007 evaluated the consequence of excessive cleavage of  $\text{Na}_V\beta2$  in overexpressing BACE1 transgenic mice, they found an surplus expression of  $\text{Na}_V1.1$ . However,  $\text{Na}_V1.1$  is intracellularly retained, doesn't translocate on the cellular membrane leading to reduced surface levels. Owing to this evidence, Corbett and colleagues demonstrated that AD Tg2576 mice, which express high levels of BACE1, exhibited increased  $\text{Na}_V\beta2$  cleavage, intracellularly retention and reduction of surface expression of  $\text{Na}_V1.1$  in cortex of APP mice, like in BACE1 transgenic mice, and spike-wave discharges and abnormal neuronal activity.

In addition to expression changes of one or more  $\text{Na}_V$  subunits, it is possible that  $\text{A}\beta$  can induce neuronal circuit hyperactivity increasing  $\text{Na}_V$  current density. In agreement with this possibility, antiepileptic drugs that block sodium channel activity are effective in reducing epileptiform discharges in mouse model of AD (Ziyatdinova *et al.*, 2011). Moreover, it has been demonstrated

that acute (1-2 min) application of soluble  $A\beta_{1-42}$  leads to alterations of spontaneous firing in CA1 pyramidal neurons. Moreover, authors proved that acutely exposure to  $A\beta_{1-42}$  also increased density of persistent sodium currents and these current are responsible of CA1 pyramidal neuron hyperactivity (Shuan-cheng Ren *et al.*, 2014). Nevertheless, they didn't investigate the cellular mechanisms by which  $A\beta_{1-42}$  can rapidly upregulate persistent sodium currents; they only supposed that  $Na_v1.6$  could be responsible of this effect.

## 2. AIM OF THE STUDY

The goal of this work was to determine the role of the Na<sup>+</sup> channel subunit Na<sub>v</sub>1.6 to the Alzheimer's Disease pathogenesis. In particular, we first sought to determine possible changes in Na<sub>v</sub> current density after the exposure to the Aβ<sub>1-42</sub> peptide in mouse wild type and in AD-related Tg2576 hippocampal neurons. Then, to assess the role of Na<sub>v</sub>1.6 subunit, we analyzed the functional contribution of Na<sub>v</sub>1.6 in the same experimental conditions in presence of *si*RNA direct against Na<sub>v</sub>1.6 mRNA or of Anisomycin that promotes p38 MAP Kinase-mediated Na<sub>v</sub>1.6 endocytosis.

### 3. MATERIALS AND METHODS

#### 3.1 Drugs And Chemicals

A $\beta$ <sub>1-42</sub>, Poly(D)-lysine Hydrobromide Mol Wt 30,000-70,000 (P7280), Poly(D)-lysine Hydrobromide Mol Wt >300,000 (P7405), Cytosine  $\beta$ -D-arabinofuranoside (Ara-C), Anisomycin and mouse monoclonal anti- $\beta$ -Tubulin, as well as all other materials for solution preparation, were from Sigma Aldrich (St. Louis, MO, USA). Tetrodotoxin (TTX), rabbit polyclonal anti-Na<sub>v</sub>1.6 were from Alomone Labs (Jerusalem, Israel). Mouse monoclonal anti-MAP2 was from Sigma-Aldrich (Milan), HBSS, Eagle's MEM 10X, horse serum (HS), fetal bovine serum (FBS), L-glutamine and phosphate buffered saline (PBS) were purchased from LifeTechnologies (Oslo, Norway). Protease inhibitor cocktail II was purchased from Roche Diagnostic.

#### 3.2 Mice

Animals were kept under standard conditions of temperature, humidity and light, and were supplied with standard food and water *ad libitum*. Animals were handled in accordance with the recommendations of International Guidelines for Animal Research and the experimental protocol was approved by the Animal Care and Use Committee of "Federico II" University of Naples. All efforts were made to minimize animal suffering and to reduce the number of animal used.

Heterozygous male Tg2576 mice and wild-type littermates, obtained backcrossing male Tg2576 mice with F1 wild-type female, were used for all experiments. Tg2576 mice, purchased from commercial source [B6;SJL-

Tg(APPSWE)2576Kha, model 1349, Taconic, Hudson, NY], are well-established AD-related mouse model carrying the human APP Swedish 670/671 mutation (K670N e M671L; Hsiao *et al.*, 1996). F1 wild-type female (B6;SJL) littermates were obtained crossing female C57BL/6 with male SJL; C57BL/6 and SJL mice were purchased from Charles River.

### 3.2.1 Genotyping: PCR Analysis

Genomic DNA from mouse tails was isolated with salt precipitation method. Tails after the cut were incubated with tail digestion buffer (50 mM Tris-HCl pH 8.0, 100 mM EDTA pH 8.0, 100 mM NaCl, 1% SDS) supplemented with Proteinase K (Sigma Aldrich, Milan, Italy) at a final concentration of 0.5 mg/ml and placed in water bath at 55-60°C overnight with mixing. This step should result in the complete solubilization of the tail fragment.

Genomic DNA from mouse embryonic tissue was extracted with phenol chlorophorm method. Embryonic brain tissue was kept during cerebral dissection and frozen immediately upon collection. After thawing, same volume of Trizol Reagent (Invitrogen) was added to each sample in order to homogenize the tissue and DNA was extracted following manufacturer guideline. DNA concentration and purity of each sample was quantified using Nanodrop Spectrophotometer (Thermo Fisher Scientific, Wilmington, DE,US).

We used following primers to amplify the DNA region with human APP Swedish mutation on both types of genomic DNA: 5'-CTGACCACTCGACCAGGTTCTGGGT-3' and 5'GTGGATAACCCCTCCCCCAGCCTAGACCA-3' (Primm, Milan, Italy). 50 ng/μL of DNA were used for PCR reaction. The amplification protocol (30

cycles) was the following: 95°C for 45 s, 55°C for 60 s, 72°C for 60 s. Each 25- $\mu$ L reaction contained: 1U of AmpliTaq DNA Polymerase (Lucigen, US) and 0.5  $\mu$ M of each primer. The amplification products were visualized on agarose (2%) gel electrophoresis by loading approximately half (10  $\mu$ L) of each reaction per lane. The band of 466bp indicated the transgenic genotype, whereas its absence indicated the wild type genotype.

### **3.3 Mouse Hippocampal Cell Cultures**

Primary neuronal cultures were prepared from hippocampi of embryonic day (E) 16 Tg2576 and wild-type littermate mice. Embryonic age (E) was calculated by considering E0.5 the day when a vaginal plug was detected. Briefly, pregnant animals were anesthetized and sacrificed by cervical dislocation. Hippocampal tissues from embryos were dissected in ice-cold dissecting medium (HBSS supplemented with 27 mM glucose, 20 mM sucrose, 4 mM sodium bicarbonate), centrifuged, and the resulting pellet was mechanically dissociated with a fire polished glass pipette. Cells were resuspended in plating medium consisting in Eagle's MEM (MEM, Earle's salts, supplied bicarbonate-free) supplemented with 5% fetal bovine serum, 5% horse serum, 2 mM L-glutamine, 20 mM glucose, 26 mM bicarbonate, and plated on 35mm culture dishes or onto 18 mm glass coverslips (Glaswarenfabrik Karl Hecht KG, Sondheim, Germany) coated with 100  $\mu$ g/ml poly(D)-lysine at a density of one embryo hippocampi/1 ml. Three days after plating, non-neuronal cell growth was inhibited by adding 10 $\mu$ M of cytosine arabinofuranoside. 24 hours after this treatment, the planting medium was replaced by growth medium (Eagle's Minimal Essential Medium with 20 mM glucose, 26 mM NaHCO<sub>3</sub> supplemented with 2mM L-glutamine and 10% horse serum. Neurons were

cultured at 37°C in a humidified 5% CO<sub>2</sub> atmosphere. All the experiments were performed between 8-16 days *in vitro* DIV.

### **3.4 A $\beta$ Oligomers Preparation And Cellular Treatments**

A $\beta$ <sub>1-42</sub> oligomers were made according to the method described by Pannccione *et al.* (2012). Briefly, lyophilized A $\beta$ <sub>1-42</sub> synthetic peptides were dissolved in PBS to obtain a 1 mM stock solution, incubated for 48 hours at 37°C to pre-aggregate the peptide, and stored at -20°C (Lorenzo and Yankner, 1994). Before all experiments, we tested a pre-aggregated preparation of the A $\beta$ <sub>1-42</sub>. SDS-PAGE was performed using monoclonal antibody 4G8 (Sigma Aldrich, Milan, Italy), which recognizes an epitope within residues 1-17 of human A $\beta$ . Results showed that the oligomers between 18 and 32 kDa were the major species of A $\beta$ <sub>1-42</sub> peptide in the preparation (data not shown).

A $\beta$ <sub>1-42</sub> exposure was carried out in growth medium at the final concentration of 5  $\mu$ M. When we performed time-course experiments, the A $\beta$ <sub>1-42</sub> was added to culture medium at above mentioned concentration for 10 minutes, 1, 24, 48 and 72 hours and kept throughout the experiment.

### **3.5 Anisomycin Treatment**

Tg2576 and wild type hippocampal neurons grown on glass coverslips for 12 and 15 DIV were pretreated for 30 minutes at 37°C in a humidified 5% CO<sub>2</sub> atmosphere with 10  $\mu$ g/ml Anisomycin (Sigma Aldrich), a specific activator of MAP p38 $\alpha$ . For electrophysiological experiments, at the end of the pre-treatment the culture medium was replaced with the bath solution. Same protocol was used for immunocytochemistry analysis.

### 3.6 Western-blot analysis

Hippocampal neurons from Tg2576 and wild-type mice were washed thoroughly to remove medium using PBS. To obtain total lysates for immunoblotting analysis, neurons were scraped in ice-cold RIPA buffer (50 mM Tris-HCl (pH 7.4), 1% Triton X-100, 0.25% sodium deoxycholate, 150 mM NaCl, 5 mM MgCl<sub>2</sub>, 1 mM EDTA, 0.1% SDS, Protease Inhibitor Cocktail II), sonicated, incubated for 1 hour on ice and centrifuged at 12000g at 4 °C for 30 min. The total protein content of resulting supernatant was determined using the Bradford reagent.

Hippocampal tissues from Tg2576 and wild-type were homogenized in a glass teflon grinder (10 strokes at 500 rpm in about 1 min) using a lysis buffer containing (in mM): 250 sucrose, 10 KCl, 1.5 MgCl<sub>2</sub>, 1 EDTA, 1 EGTA, 1 dithiothreitol, 20 HEPES, pH 7.5, (Angulo *et al.* 2004) and completed with Protease Inhibitor Cocktail II. Tissue suspensions were then sonicated and incubated for 1 hour on ice. After centrifugation at 12,000 g at 4 °C for 5 min, the supernatants were collected. The protein content of resulting supernatant was determined using the Bradford reagent.

70 µg of proteins were mixed with a Laemmli sample buffer; then, they are applied and resolved on 10% SDS-PAGE polyacrylamide gels. Following transfer onto nitrocellulose membranes (Hybond-ECL, Amersham Bioscience, UK), non-specific binding sites were blocked by incubation for 2 hrs at 4°C with 5% non-fat dry milk (Bio-Rad Laboratories, Milan, Italy) in TBS-T buffer; subsequently, incubated with primary antibodies overnight at 4°C. After three 10-min washes with TBS-T, the membranes were incubated 1 h with the appropriate secondary antibody. Excessive antibodies were then washed away

three times (10 min) with TBS-T. Immunoblots were visualized by enhanced chemiluminescence (ECL) (Amersham-Pharmacia-Biosciences, UK). Films were developed using a standard photographic procedure and the relative levels of immunoreactivity were determined by densitometry using ImageJ Software (NIH, Bethesda, MA, USA).

Primary antibodies used were: rabbit-polyclonal antibody anti-Nav1.6 and rabbit-polyclonal antibody anti-Navβ1 (1:1000; Alomone Labs); rabbit-polyclonal anti-p38α antibody (1:1000; Santa Cruz Biotechnology); mouse monoclonal anti-tubulin (1:3000; Sigma Aldrich).

### **3.7 Electrophysiological recordings**

Transient Na<sup>+</sup> currents ( $I_{TNa}$ ) were recorded, by patch-clamp technique in whole-cell configuration, in the following groups of hippocampal neuronal cultures: (a) wild-type, (b) wild-type+Aβ<sub>1-42</sub>, (c) wild-type+Anisomycin (d) Tg2576, (e) Tg2576+Anisomycin. Hippocampal neurons were plated on 25-mm glass coverslips for recording. Currents were filtered at 5 kHz and digitized using a Digidata 1322A interface (Molecular Devices). Data were acquired and analyzed using the pClamp software (version 9.0, Molecular Devices).

All recordings were performed at room temperature (20-21°C). The total inward Na<sup>+</sup> current was measured by applying, from a holding potential of -70 mV, depolarizing voltage steps of ....ms duration ranging from -70 to +50 mV. These were preceded by conditioning pulses at -100 mV lasting for .. s to allow full recovery from  $I_{Na}$  inactivation. Possible changes in cell size occurring after specific treatments were calculated by monitoring the capacitance of each cell

membrane, which is directly related to membrane surface area, and by expressing the current amplitude data as current densities (pA/pF). The capacitance of the membrane was calculated according to the following equation:  $C_m = \tau_c \cdot I_0 / \Delta E_m (1 - I_\infty / I_0)$ , where  $C_m$  is the membrane capacitance,  $\tau_c$  is the time constant of the membrane capacitance,  $I_0$  is the maximum capacitance current value,  $\Delta E_m$  is the amplitude of the voltage step, and  $I_\infty$  is the amplitude of the steady-state current.

The neurons were perfused with External Ringer solution contained (in mM): NaCl 126, NaHPO<sub>4</sub> 1.2, KCl 2.4, CaCl<sub>2</sub> 2.4, MgCl<sub>2</sub> 1.2, glucose 10 and NaHCO<sub>3</sub> 18, TEA 20, and nimodipine 10  $\mu$ M (pH 7.4). The pipette solution contained (mM): Kgluconate 145, Mg-ATP 1, and 0.1 CaCl<sub>2</sub>, 2 MgCl<sub>2</sub>, 0.75 EGTA, HEPES 10, pH 7.3. TEA was included to block delayed outward rectifier K<sup>+</sup> components; nimodipine (10  $\mu$ M) was added to external solution to block L-type Ca<sup>2+</sup>-channels. TTX (50 nM) was added to the bath solution to isolate components of Na<sup>+</sup>-currents flowing through TTX-sensitive Na<sup>+</sup> channels.

### **3.8 Immunocytochemistry in hippocampal neurons**

Hippocampal neurons obtained from Tg2576 and wild type mice were washed in cold PBS and fixed in 4% (w/v) paraformaldehyde in PBS for 40 minutes at room temperature. After four 10-min washes in PBS, the cells were first pre-incubated in PBS containing 3% (w/v) bovine serum albumin (Sigma, Milan, Italy) for 60 minutes and then with the primary anti-Na<sub>v</sub>1.6 polyclonal antibody (1:1000) and primary anti-MAP2 monoclonal antibody (1:1000) at 4° C overnight. Next, cells were washed in PBS and, for double

immunofluorescence, were instead incubated in a mixture of fluorescent labeled secondary antibodies (Alexa 488- or Alexa 594- conjugated anti-mouse or anti-rabbit IgGs) for 1h at room temperature. Cell nuclei were stained with Hoechst (Sigma, Milan, Italy). After the final wash, cells were mounted and coverslipped with Vectashield (Vector Labs, Burlingame, CA,). Slides were analysed with a confocal microscope (Zeiss, Nikon Instruments, Florence, Italy) equipped with a CCD digital camera (Coolsnap-Pro, Media Cybernetics, Silver Springs, MD, USA) and Image Pro-Plus software (Media Cybernetics, Silver Springs, MD, USA).

### **3.9 Na<sub>v</sub>1.6 Silencing RNA Transfection**

Small interfering RNA (siRNA) against Na<sub>v</sub>1.6 and the validated nonsilencing AllStars negative control siRNA that has no homology to any known mammalian gene were purchased from Qiagen (Milan, Italy). Two different predesigned siRNAs directed against mouse SCN8a transcript (GenBank accession number NM\_001077499; Entrez Gene ID 20273) were tested: Mm\_Scn8a\_5 Flexitube siRNA (Cat.No. SI02671277) and Mm\_Scn8a\_6 Flexitube siRNA (Cat.No SI02713956), which bound two different coding sequences on Na<sub>v</sub>1.6 mRNA downstream of the transcription start site. The siRNAs were transiently transfected using HiPerFect Transfection Reagent (Qiagen) at a final concentration of 50 nM in serum free OptiMEM medium for 5 hours, at the end of which OptiMEM was replaced by growth medium.

Wild type hippocampal neurons were used for siRNA transfection experiments; the gene-silencing efficiency of siRNA was determined 48 hrs after transfection by electrophysiological measurements.

### **3.10 Statistical Analysis**

Statistical analysis were performed with ANOVA followed by Newman test or Student t-test. Differences were considered to be statistically significant at  $p < 0.05$ .

## 4. RESULTS

### 4.1 $A\beta_{1-42}$ exposure raised $Na_v$ functional activity in hippocampal neurons

We first examined whether  $A\beta_{1-42}$  peptide effected sodium current density e/o kinetics in hippocampal neurons recording sodium currents by patch-clamp technique in whole-cell configuration. To this purpose, we exposed hippocampal neurons to  $A\beta_{1-42}$  peptide for different time, (10 minutes, 1, 24, 48, and 72 hours. Time-course experiments revealed that the exposure to 5  $\mu$ M  $A\beta_{1-42}$  didn't immediately modify  $Na_v$  channels activity, as observed from electrophysiological recordings after 10 minutes exposure. On the other hand, 24 and 48 hrs of  $A\beta_{1-42}$  treatment induced a significant increase of  $Na^+$  current density, followed by a return to basal levels at 72 hours (Fig. 5A and 15). These currents were completely inhibited by the extracellular application of the selective sodium channel blocker TTX (50 nM) in control conditions and after exposure to 5  $\mu$ M  $A\beta_{1-42}$  (Fig. 5D) indicating that this  $Na^+$ -influx is mediated by TTX-sensitive voltage-gated sodium channels.

Interesting, when we analysed the I–V-relationships for endogenous sodium currents in control and  $A\beta_{1-42}$ -treated hippocampal neurons, we observed that  $A\beta_{1-42}$ - exposure not only increased the peak current but also modified the kinetics of  $Na_v$  channels. In fact, 24 hrs  $A\beta_{1-42}$  treatment caused a significant leftward shift in the voltage dependence of activation: in fact, the peak current of  $Na^+$  currents occurred at -20 mV in the  $A\beta_{1-42}$ -exposed neurons respect -10 mV in the control (Fig. 5C). Interesting, in accordance with the

time-course experiments, at 48 and 72 hours  $A\beta_{1-42}$  exposure we observed that the progressive reduction of the peak current was associated with no significant changes in the voltage dependence of activation (Fig. 5C).

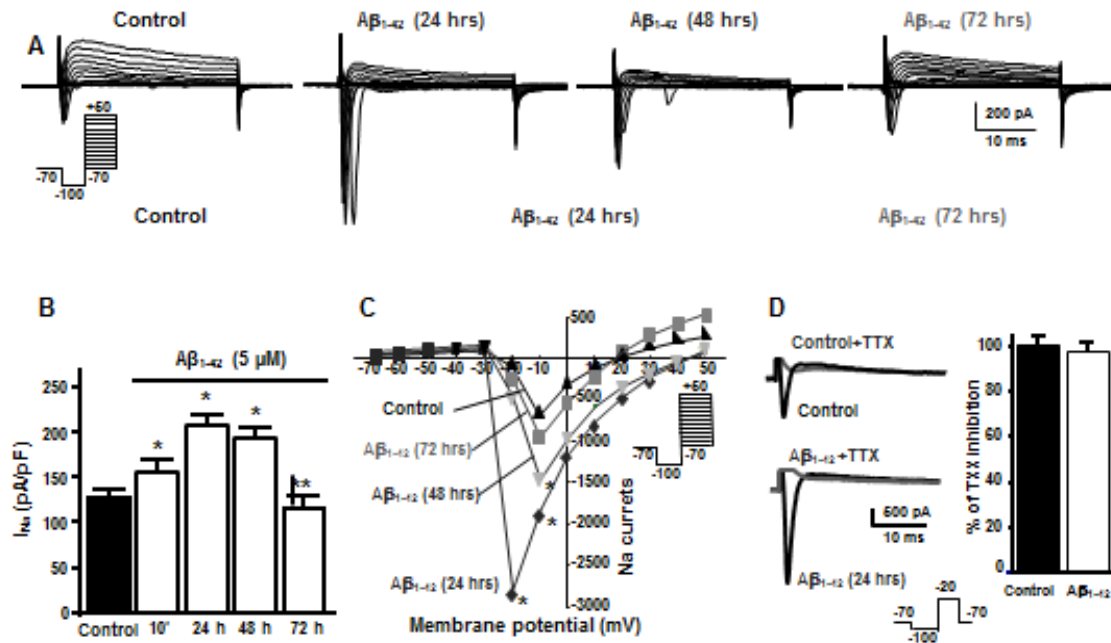


**Figure 5.  $A\beta_{1-42}$  exposure raised  $Na_v$  functional activity in hippocampal neurons.** (A)  $I_{Na}$  traces recorded under control conditions and after exposure to  $A\beta_{1-42}$  for different time. (B) Quantification of  $I_{Na}$  represented in A. (C) I-V-relationships for endogenous sodium currents in control and  $A\beta_{1-42}$ -treated hippocampal neurons. (D)  $I_{Na}$  traces recorded under control conditions and after  $A\beta_{1-42}$  exposure in presence of TTX and relative percentage of TTX-induced  $I_{Na}$  inhibition. All values are expressed as mean  $\pm$  SEM of current densities in 3 independent experimental sessions (\*  $p < 0.05$  versus respective controls).

## 4.2 $A\beta_{1-42}$ fails to increase $Na^+$ currents in $Na_v1.6$ silenced mouse hippocampal cultures

In order to test which is the contribution of  $Na_v1.6$  activity to the  $A\beta_{1-42}$  effects on  $Na_v$  currents, we explored the effects of selective knockdown of this subunit on the sodium currents recorded after the exposure to beta-amyloid peptide.

To this aim, we performed silencing experiments of  $Na_v1.6$ . Firstly, we tested the silencing efficiency of two different  $Na_v1.6$  siRNAs, the Mm\_Scn8a\_5

and Mm\_Scn8a\_6, both at the concentration of 50 nM, transfecting wild type hippocampal neuronal cultures. Patch clamp experiments revealed that Mm\_Scn8a\_6 siRNA was more effective than Mm\_Scn8a\_5 to knock down Nav1.6 as revealed from the significant reduction of the Na<sup>+</sup> currents (Fig. 6A and 6B). Then, we used Mm\_Scn8a\_6 siRNA to silence Nav1.6 expression before the exposure to Aβ<sub>1-42</sub>. Interestingly, knocking down of this sodium channel subunit before Aβ<sub>1-42</sub>-treatment (24 hours) counteracted the Na<sub>v</sub> currents increase (Fig. 6D and 6E).

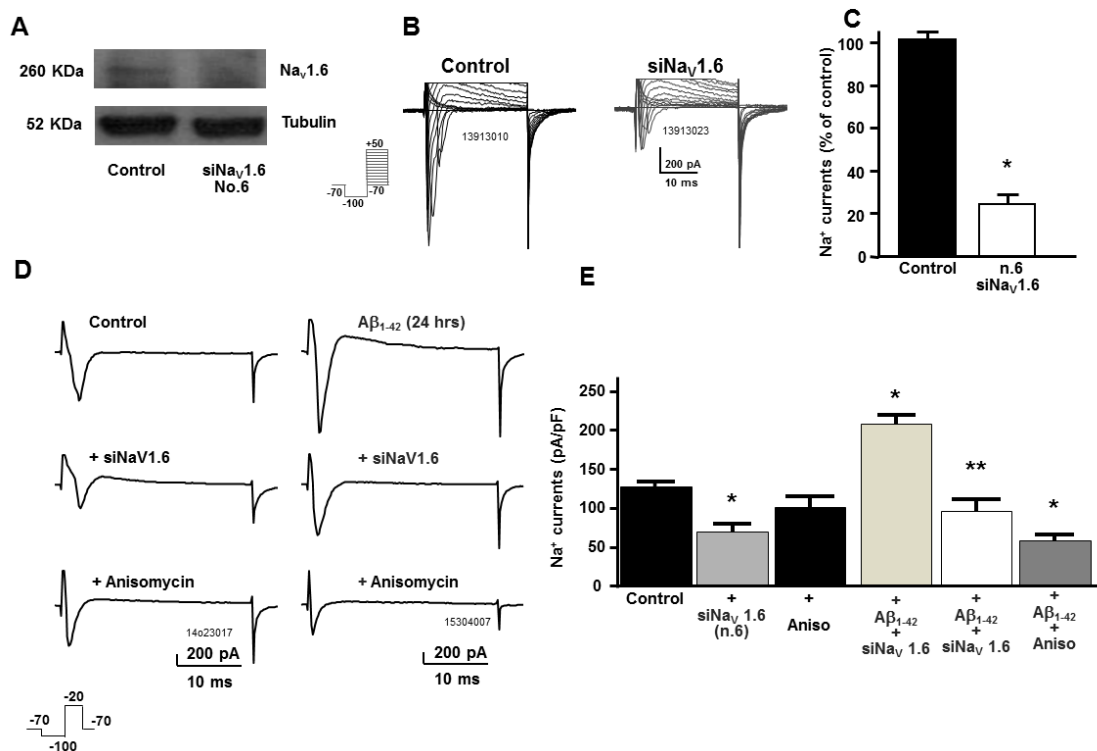


**Figure 6** Aβ<sub>1-42</sub> fails to increase Na<sup>+</sup> currents in Nav1.6 silenced mouse hippocampal cultures. (A) Nav1.6 protein levels under control conditions and after siRNA transfection (B) I<sub>Na</sub> traces recorded under control conditions and after siRNA transfection. (C) Quantification of I<sub>Na</sub> represented in B. (D) I<sub>Na</sub> traces recorded under control conditions and after Aβ<sub>1-42</sub> exposure after siRNA transfection or Anisomycin treatment. (E) Quantification of I<sub>Na</sub> represented in D. All values are expressed as mean ± SEM of current densities in 3 independent experimental sessions (\* p<0.05 versus respective controls).

### **4.3 pp38-mediated internalization of Na<sub>v</sub>1.6 counteracts A $\beta$ -induced I<sub>Na</sub><sup>+</sup> increase**

To confirm that the increased density of I<sub>Na</sub> in the wild-type hippocampal neurons exposed to A $\beta$ <sub>1-42</sub> for 24 hours is mainly due to Na<sub>v</sub>1.6  $\alpha$ -subunit, we added Anisomycin (10 $\mu$ g/mL) for 30 minutes at culture medium hippocampal neurons before recording sodium currents. Anisomycin is an antibiotic that is routinely used to activate p38 MAP kinases (Cano and Mahadevan, 1995). *Wittmack et al.* (2005) have been demonstrated that Anisomycin-activated  $\alpha$ -pp38 phosphorylates Na<sub>v</sub>1.6 at a single serine residue (Ser553) within the sequence motif Pro-Gly-Ser553-Pro in loop 1 (Nav1.6/L1). This phosphorylation reduces selectively Na<sub>v</sub>1.6 current density because decreases the number of available channels by internalization of this channel.

In agreement with results of silencing experiments, patch clamp recordings revealed that Anisomycin-induced activation of p38 $\alpha$  was able to prevented I<sub>Na</sub> increase in wild-type hippocampal neurons exposed to A $\beta$ <sub>1-42</sub> peptide. More interestingly, as pp38 $\alpha$  promoted only Na<sub>v</sub>1.6 endocytosis, the reduction observed of total Na<sup>+</sup> current density indicated that Na<sub>v</sub>1.6 significantly contributes to A $\beta$ <sub>1-42</sub>-induced I<sub>Na</sub><sup>+</sup> enhancement (Fig 6D and 6E).

### **4.4 Increased Na<sub>v</sub> Activity In Hippocampal Neurons Of AD Mouse Model Tg2576**

To understand whether sodium-current densities are also increased in AD, hippocampal neurons obtained from a mouse model of Alzheimer's disease, Tg2576, were used to record total sodium currents. Time-course recording experiments at different days in vitro revealed that hippocampal neurons from Tg2576 transgenic-mice displayed an early increase of Na<sup>+</sup>

current densities respect wild-type hippocampal neurons. In fact,  $\text{Na}_V$  activity was significantly increased already at 8 DIV in culture, reached the maximal value at 12 DIV, and showed a less pronounced, but still significant, increase at 15 DIV ( Fig. 7A and 7B) in the transgenic neurons respect wild-type. These results are in agreement with those obtained in the hippocampal neurons exposed to  $\text{A}\beta_{1-42}$ .

Intriguingly, analysis of the I–V-relationships for endogenous sodium currents in wild-type and Tg2576 hippocampal neurons revealed that 12 DIV in culture Tg2576 neurons displayed a significant leftward shift in the voltage dependence of activation compared to wild-type neurons, with current peak at -30mV rather than at -10 mV of wild-type neurons (Fig. 7C), suggesting that the Tg2576 hippocampal neurons have an increased number of channels open at a given voltage, consistent with an increase in the activity of the  $\text{Na}_V$  channels.

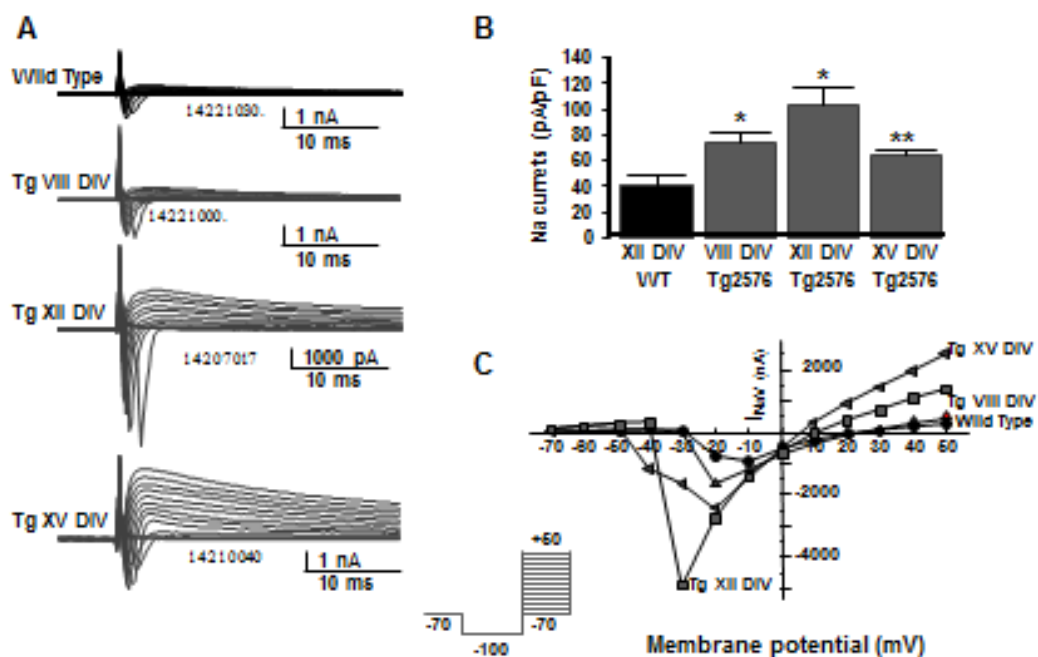


**Figure 7. (A) Increased  $\text{Na}_V$  Activity In Hippocampal Neurons Of AD Mouse Model Tg2576. (A)**  $I_{\text{Na}}$  traces recorded in wild type and Tg2576 hippocampal neurons at different time

in culture. **(B)** Quantification of  $I_{Na}$  represented in A. **(C)** I–V-relationships for endogenous sodium currents in wild type and Tg2576 hippocampal neurons. All values are expressed as mean  $\pm$  SEM of current densities in 3 independent experimental sessions (\*  $p < 0.05$  versus respective controls).

#### **4.5 The Anisomycin-stimulated $Na_v1.6$ endocytosis prevents increase of $I_{Na}^+$ currents in hippocampal neurons of Tg2576 mice**

To examine whether also in the hippocampal neurons of the Tg2576 mice the increased density of  $I_{Na}$  is mainly due to  $Na_v1.6$   $\alpha$ -subunit, as in the hippocampal neurons exposed to  $A\beta_{1-42}$ , we exposed control and Tg2576 hippocampal neurons to Anisomycin (10 $\mu$ g/mL) for 30 minutes before recording sodium currents. We observed that Anisomycin induced a significant reduction of sodium currents in Tg2576 hippocampal neurons respect untreated transgenic neurons, comparable to those recorded in untreated wild type neurons (Fig. (8A and 8B), indicating that the increase of  $Na_v1.6$  peak currents mainly contribute to the increased sodium currents in transgenic hippocampal neurons.

We also examined the effects of Anisomycin on steady-state biophysical properties of  $Na_v$  currents. Interesting, the analysis of the I/V relationship of  $Na^+$  currents recorded in Anisomycin-pretreated Tg2576 hippocampal neurons revealed that the treatment counteracted the leftward shift in the voltage dependence of  $Na_v$  activation. In fact, as in the wild-type hippocampal neurons, the current peak occurred at -10mV rather than at -30mV, further supporting the hypothesis that  $Na_v1.6$  is responsible of the increased sodium current density in the transgenic hippocampal neurons (Fig. 8C).

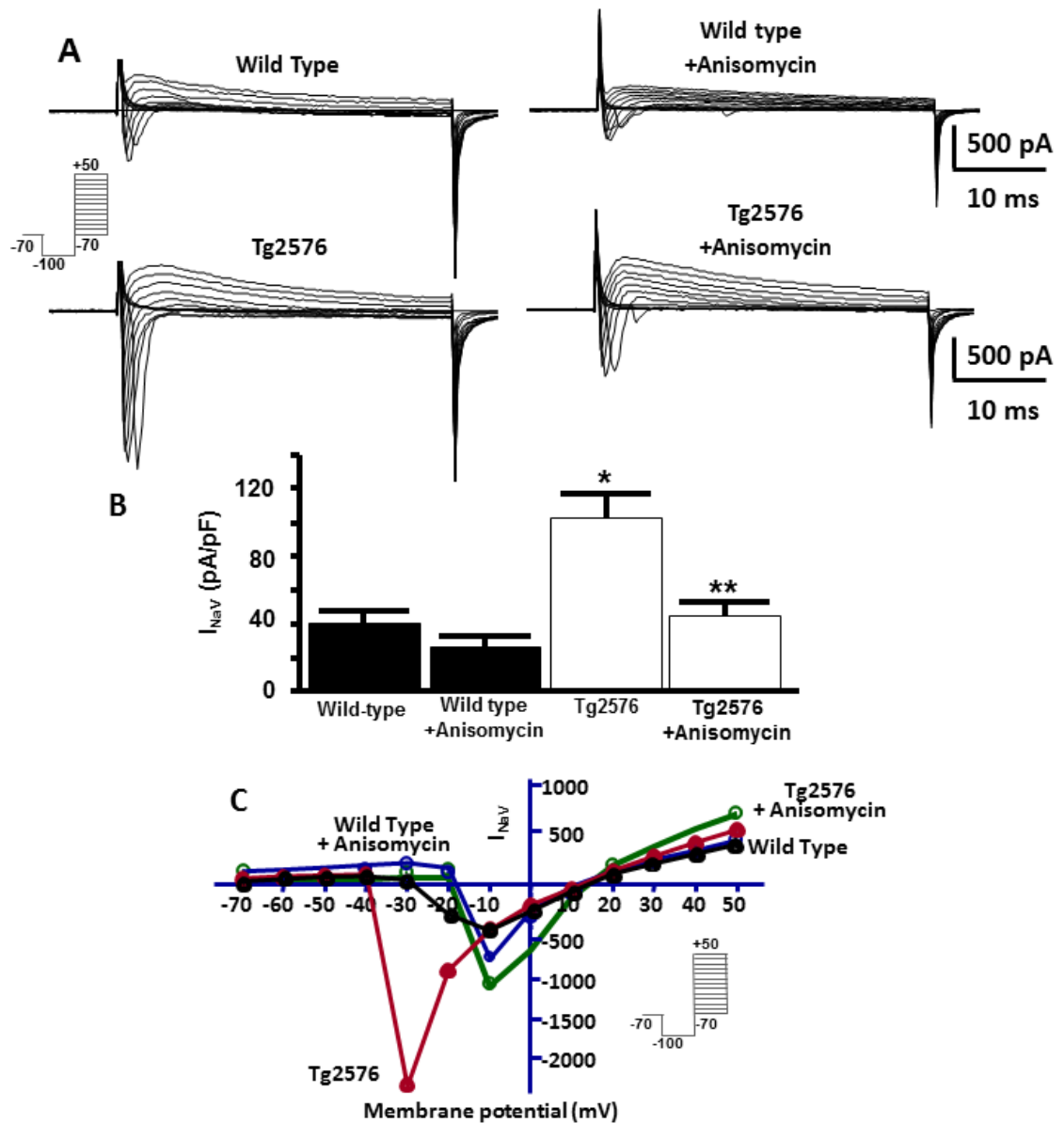


**Figure 8. The Anisomycin-stimulated  $Na_V1.6$  endocytosis prevents increase of  $I_{Na}^+$  currents in hippocampal neurons of Tg2576 mice.** (A)  $I_{Na}$  traces recorded in wild type and Tg2576 hippocampal neurons under control conditions and after treatment with Anisomycin. (B) Quantification of  $I_{Na}$  represented in A. (C) I–V-relationships for endogenous sodium currents in wild type and Tg2576 hippocampal neurons under control conditions and after treatment with Anisomycin. All values are expressed as mean  $\pm$  SEM of current densities in 3 independent experimental sessions (\*  $p < 0.05$  versus respective controls).

#### 4.6 Overexpression of $Na_V1.6$ channel subunits in Tg2576 hippocampal neurons as a neuroprotective mechanism

Because  $Na_V1.6$  activity was significantly up-regulated in Tg2576 hippocampal neurons, we measured the expression levels of this subunit in

these neurons. Immunoblot analysis performed with a Na<sub>v</sub>1.6-specific antibody on protein extracts from wild-type and Tg2576 hippocampal neurons at 12 DIV revealed one band at 260 kDa that corresponds to subunit. Densitometric analysis showed that this band was considerably more intense in hippocampal neurons of Tg2576 than in the controls (Fig. 9A).

Immunocytochemical analysis, performed with the same anti-Na<sub>v</sub>1.6 antibody, confirm raised expression of Na<sub>v</sub>1.6 in Tg2576 hippocampal neurons respect in wild type. More interestingly, Nav1.6 immunosignal pattern was more different between wild type and Tg2576 cultured hippocampal neurons; in fact, we observed a plasma membrane localization and a punctuated staining pattern mostly confined throughout the neuropil in wild type hippocampal neurons, whereas, in Tg2576 hippocampal cells, the Na<sub>v</sub>1.6 immunosignal was more confined to the soma plasma membrane (Fig. 9B).

Moreover, to confirm that the reduction of total sodium current observed in Tg2576 hippocampal neurons after the treatment with Anisomycin is due to decreased levels of Na<sub>v</sub>1.6, immunocytochemical experiments were performed in Anisomycin-treated wild type and Tg2576 hippocampal neurons. Interestingly, Na<sub>v</sub>1.6 immunosignal is significantly reduced in both neuronal cultures, confirming that pharmacological stimulation of Na<sub>v</sub>1.6 endocytosis abolishes sodium current increase. Moreover, Anisomycin-induced Na<sub>v</sub>1.6 internalization had different effects in wild type and Tg2576 hippocampal neurons. In fact, Anisomycin rapidly induced numerous beads in most neurites of transgenic hippocampal neurons compared with wild type cells, in which no morphological changes were observed. The appearance of focal bead-like swellings in the dendrites and axons as a consequence of Na<sub>v</sub>1.6 sodium

channel density reduction at the plasma membrane reflected neurite damage and indicated that most likely overexpression of this sodium channel subunit could be a protective mechanism against  $A\beta_{1-42}$  toxic effects (Fig. C).

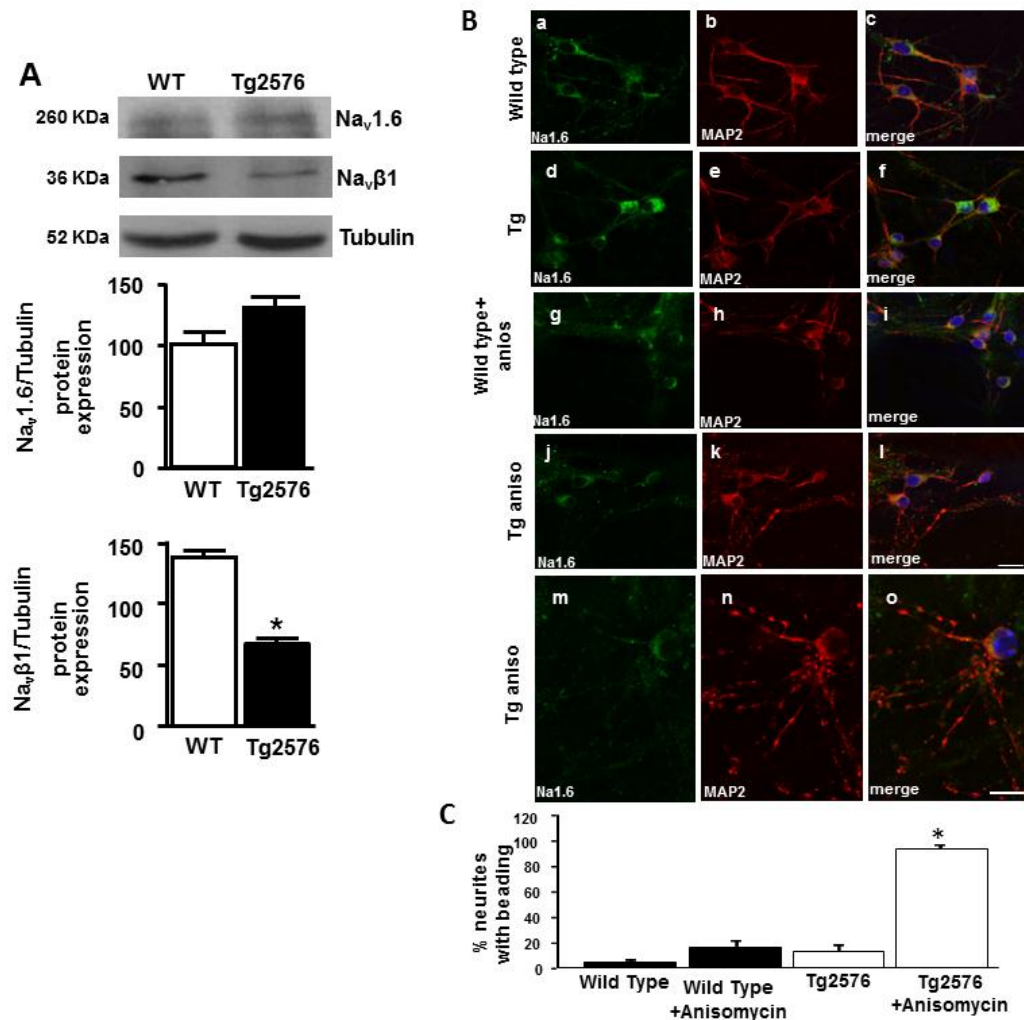


**Figure 9. Na<sub>v</sub>1.6 and Na<sub>v</sub>β1 Auxiliary Subunit expression in Tg2576.** (A) Immunoblotting analysis of Na<sub>v</sub> 1.6 and Na<sub>v</sub>β1 and densitometric analysis in Wild Type and Tg2576 hippocampal neurons. (B) immunocytochemical analysis of Na<sub>v</sub>1.6 signal in Wild Type and Tg2576 hippocampal neurons, without or after treatment with Anisomycin. (C) Quantification of neuritic beading observed in B. All values are expressed as mean ± SEM of optic densities in 3 independent experimental sessions (\* p<0.05 versus respective controls).

#### 4.7 Reduced Expression Of Na<sub>v</sub>β1 Auxiliary Subunit In Tg2576 Hippocampal Neurons

To investigate which mechanism could be responsible of leftward shift in the voltage dependence of Na<sub>v</sub> current activation, we measured the expression

levels of  $\text{Na}_v\beta 1$  auxiliary subunit because it has been demonstrated that  $\beta 1$  subunit has modulatory effects on the kinetics and gating of  $\text{Na}_v 1.6$  sodium channels, in particular co-expression of  $\text{Na}_v 1.6$  and  $\text{Na}_v\beta 1$  determines depolarizing shift in the midpoint potential for channel activation (Bingjun He and David M. Soderlund, 2014). To this aim, we analyzed  $\text{Na}_v\beta 1$  protein levels in cellular lysates of wild-type and Tg2576 hippocampal neurons at 12 DIV. Western blotting analysis revealed a significant decrease in the optical density of the 36kDa ( $\text{Na}_v\beta 1$ ) specific bands in hippocampal neurons of Tg2576 respect wild type (Fig. 9A).

## 5. DISCUSSION

The results of the present study provide the first evidence that Na<sub>v</sub>1.6 channel subunit is involved in AD etiopathogenesis. In hippocampal neurons A $\beta$ <sub>1-42</sub> induced a time-dependent upregulation of Na<sup>+</sup> currents with a peak at 24 hours. Similarly, Tg2576 hippocampal neurons displayed a Na<sup>+</sup> current upregulation with a peak at XII DIV. This enhancement was selectively mediated by Na<sub>v</sub>1.6 channel isoform. In fact, the removal of Na<sub>v</sub>1.6 isoform either by Na<sub>v</sub>1.6 silencing or the pharmacological pretreatment with Anisomycin, as well known activator of stress-related p38 MAPK (X. Guo *et al.* 2011), prevented this increase. Moreover, Na<sub>v</sub>1.6 augmented activity was due to the reduction of its auxiliary subunit  $\beta$ 1 protein expression. By contrast, in the late phase, at 72 hours after A $\beta$ <sub>1-42</sub> or in hippocampal neurons at XV DIV Tg2576, the Na<sup>+</sup> currents decreased and were comparable to the respectively controls.

It is well known that Na<sub>v</sub>1.6 is the major isoform at nodes of Ranvier in myelinated axons and, additionally, is distributed along unmyelinated C-fibers of sensory neurons and is expressed in presynaptic and postsynaptic membranes of the neocortex and cerebellum (Caldwell *et al.*, 2000). This pattern of expression implies that Na<sub>v</sub>1.6 sodium channels play important roles in both electrical and chemical signaling in the brain. Na<sub>v</sub>1.6 currents might significantly impact axonal conduction and may significantly contribute to the pathophysiology of the injured nervous system such as multiple sclerosis (Black *et al.* 2007; Craner MJ, 2004 and 2005). Recently, several mutations in Na<sub>v</sub>1.6 encoding gene are been identified in patients affected by epilepsy (Estacion M *et al.*, 2014).

It has been suggested an involvement of  $\text{Na}_V1.6$  channel subunit in AD since Mukhamedyarov MA *et al.* (2009) found that  $\text{A}\beta_{1-42}$ -induced depolarization is driven by increased  $\text{Na}^+$ -influx to muscle fibers through TTX-sensitive  $\text{Na}^+$ -channels but the exact molecular mechanism is yet unknown. Interestingly, in the present study we observed a time-dependent modulation of  $\text{Na}^+$  currents. In the early phase of AD we observed an enhanced activity of  $\text{Na}_V$  channels. In fact, we observed an upregulation of  $\text{Na}^+$  currents both in hippocampal neurons exposed to  $\text{A}\beta_{1-42}$  or Tg2576 hippocampal neurons with a peak at 24 hours or at XII DIV, respectively. Moreover, this  $\text{Na}^+$  current upregulation was associated with a significant negative shift in the peak of activation of the  $\text{Na}^+$  currents of -10 mV in  $\text{A}\beta_{1-42}$  exposed hippocampal neurons or of -20 mV in Tg2576 hippocampal neurons. By contrast, in the late phase, at 72 hours after  $\text{A}\beta_{1-42}$  or in hippocampal neurons at XV DIV Tg2576, when the  $\text{Na}_V1.6$  currents abruptly decreased returning at control values, no negative shift in the peak of activation was observed. It is well known that distal end of the AIS is the preferred site for action potential initiation in cortical pyramidal neurons because of its high  $\text{Na}_V$  channel density. In particular, low-threshold  $\text{Na}_V1.6$  and high-threshold  $\text{Na}_V1.2$  channels are preferentially accumulate at the distal and proximal AIS, respectively. Patch-clamp recording in neurons revealed a high density of  $\text{Na}^+$  current and a progressive reduction in the half-activation voltage (up to 14 mV) with increasing distance from the soma at the AIS. Moreover, recent evidence show that distal  $\text{Na}_V1.6$  promotes action potential initiation, whereas proximal  $\text{Na}_V1.2$  promotes its backpropagation to the soma (Hu W, *et al* 2009). On this basis it was possible to speculate that the upregulation of  $\text{Na}^+$  currents that occurred in our experimental conditions could

be due to an increased activity of Na<sub>v</sub>1.6 channel subunits. Interestingly, the removal of Na<sub>v</sub>1.6 channel subunits by silencing directed against Na<sub>v</sub>1.6 was able to prevent the upregulation of Na<sup>+</sup> currents observed in hippocampal neurons exposed to Aβ<sub>1-42</sub> such as in Tg2576 hippocampal neurons. Moreover, the pretreatment with Anisomycin, as well known activator of stress-related p38 MAPK (Guo X. *et al.* 2011 Neuroscience) was able to counteract the upregulation of Na<sub>v</sub>1.6 activity both in hippocampal neurons exposed to Aβ<sub>1-42</sub> and in Tg2576 hippocampal.

It is well known that phosphorylation provides a fast post-translational modification of proteins that has been shown to regulate the acute response of cells to a variety of stimuli and that phosphorylation of Na<sub>v</sub> channels has been shown to produce rapid modulation of Na<sup>+</sup> currents. This phenomenon seems closely mediated by mitogen-activated protein kinases (MAPK). MAPKs are expressed in neurons and are activated in several pathological conditions including AD. In mammalian cells, three principle MAPK pathways, including ERK, JNK, and p38 MAPK, have been identified. In particular, p38 MAPK pathway is especially relevant to the response of environmental stress and inflammatory stimuli (Saklatvala, 2004 and Kumar *et al.*, 2003). Moreover, in AD brain, increased levels of activated p38 MAPK are detected and associated with neuropil threads, and neurofibrillary tangle-bearing neurons (Hensley *et al.*, 1999 and Sun *et al.*, 2003). In AD transgenic mice, p38 MAPK is significantly activated in microglia, astrocytes and neurons, around and distant from the plaques, which indicates the possible involvement of stress-related signaling pathways during the pathogenesis of AD (Hwang *et al.*, 2004, Hwang *et al.*, 2005 and Giovannini *et al.*, 2008). In addition, it has been demonstrated that

the activator of stress-related p38 MAPK, anisomycin, could induce A $\beta$  overproduction by transcriptional activation of APP, BACE1, and PS1 genes through DNMT-dependent hypomethylation and histone H<sub>3</sub> hyperacetylation suggesting the involvement of epigenetic mechanism by which oxidative stress contributes to the pathogenesis of AD (Guo *et al.* 2011). Interesting, sequence analysis shows that Na<sub>v</sub>1.6 contains a putative MAPK recognition module in the cytoplasmic loop. Moreover, it has been demonstrate that Na<sub>v</sub>1.6 channels and p38 MAPK colocalize in rat brain tissue and that activated p38 phosphorylates Na<sub>v</sub>1.6, specifically at serine 553 (S553) significant and selective reducing peak Na<sub>v</sub>1.6 current amplitude (Wittmack *et al.* 2005).

The immunoblot and immunocytochemical analysis, performed with the selective anti-Na<sub>v</sub>1.6 antibody, confirmed that this enhanced Na<sub>v</sub>1.6 activity was associated to Na<sub>v</sub>1.6 protein expression upregulation. In particular, immunocytochemical analysis revealed a pronounced perikaryal staining intensely confined to the soma plasmamembrane in Tg2576 hippocampal neurons whereas in wild type neurons this signal was a punctuated staining pattern mostly confined throughout the neuropil and less intense. Moreover, in the presence of Anisomycin Na<sub>v</sub>1.6 immunosignal was significantly reduced in Tg2576 hippocampal neurons in the presence of p38 activator.

The pathophysiological role played by Na<sub>v</sub>1.6 enhanced activity is almost controversial. Thus from one site the increase of Na<sub>v</sub>1.6 activity is considered neurodetrimental since cause an increase in axonal intracellular sodium through a persistent Na<sup>+</sup> currents increase that leads to membrane depolarization and further activation of Na<sub>v</sub> channels. On the other hand, the increase in axonal intracellular sodium promotes the reversal of Na<sup>+</sup>/Ca<sup>2+</sup>

exchanger that plays a neuroprotective action during AD in the early phase (Pannaccione *et al.* 2012). Immunocytochemical analysis performed in the presence of Anisomycin showed that the internalization of Na<sub>v</sub>1.6 seemed to play a detrimental role. In fact, Tg2576 hippocampal neurons exposed to Anisomycin displayed an enhanced number of neurites with beading. Neuritic beading, focal bead-like swellings in the dendrites and axons, is a neuropathological sign in epilepsy, trauma, ischemia, aging, and neurodegenerative diseases such as AD (Hideyuki Takeuchi, Tetsuya Mizuno, Guiqin Zhang, Jinyan Wang, Jun Kawanokuchi, Reiko Kuno, and Akio Suzumura 2005 JBC Vol. 280, No. 11, Issue of March 18, pp. 10444 –10454). Several previous studies report that neuritic beading is a reversible response to neurotoxic stimuli independent of neuronal death. By contrast, a recent study demonstrate that dendritic beading correlates with disease severity in experimental autoimmune encephalomyelitis rat spinal cord (Zhu, B., Luo, L., Moore, G. R., Paty, D. W., and Cynader, M. S. (2003) *Am. J. Pathol.* 162, 1639-1650), suggesting that beading paralleled neuronal damage. Furthermore, the mechanisms underlying neuritic bead formation are completely unknown. Our results seemed to suggest that Na<sub>v</sub>1.6 upregulation could be involved in a neuroprotective mechanism.

Finally, western blot analysis showed that the band at ~260 kDa, corresponding to Na<sub>v</sub>1.6, was significantly higher in Tg2576 hippocampal neurons than in wild type neurons suggesting that the upregulation observed was due to an upregulation of Na<sub>v</sub>1.6 isoform. Interestingly, immunoblot analysis performed with a specific antibody against β1 auxiliary subunit of Na<sub>v</sub>1.6 isoform revealed that the band at ~36 kDa corresponding to β1

auxiliary subunit was downregulated in Tg2576 hippocampal neurons when compared to controls suggesting that this augmented activity was due to the reduction of the protein expression of  $\beta 1$  auxiliary subunit. It has been reported that  $\text{Na}_v1.6$  isoform and  $\beta 1$  auxiliary subunit in many brain regions coassemble in heteromultimeric complexes. The reciprocal interaction between the  $\text{Na}_v1.6$  and  $\beta 1$  subunits identifies a specific functional association between these two subunits that promotes neurite outgrowth, determines sodium channel localization and activity. In fact,  $\beta 1$  subunit modulates the kinetic and gating properties of  $\text{Na}_v1.6$  (Bingjun He, David M. Soderlund 2014). In particular, the voltage dependence of  $\text{Na}_v1.6$  activation, recorded in the absence of  $\beta 1$  subunits, was shifted in the direction of hyperpolarization compared to  $\text{Na}_v1.6$  recorded in the presence of  $\beta 1$  (Burbidge *et al.*, 2002; He and He and Soderlund 2011; Bingjun He, David M. Soderlund 2014).

Collectively, these results seems to demonstrate that the upregulation of  $\text{Na}_v1.6$  activity may be interpreted as a survival strategy activated by neurons in an attempt to defend themselves from the death messages triggered by this peptide during the early phase of exposure.

## 6. REFERENCES

- Abriel H**, Kamynina E, Horisberger JD, Staub O. Regulation of the cardiac voltage-gated Na<sup>+</sup> channel (H1) by the ubiquitin-protein ligase Nedd4. *FEBS Lett.* 2000 Jan 28;466(2-3):377-80.
- Alabi AA**, Bahamonde MI, Jung HJ, Kim JI, Swartz KJ. Portability of paddle motif function and pharmacology in voltage sensors. *Nature.* 2007 Nov 15;450(7168):370-5.
- Aman TK**, Grieco-Calub TM, Chen C, Rusconi R, Slat EA, Isom LL, Raman IM. Regulation of persistent Na current by interactions between beta subunits of voltage-gated Na channels. *J Neurosci.* 2009 Feb 18;29(7):2027-42.
- Aman TK**, Grieco-Calub TM, Chen C, Rusconi R, Slat EA, Isom LL, Raman IM. Regulation of persistent Na current by interactions between beta subunits of voltage-gated Na channels. *J Neurosci.* 2009 Feb 18;29(7):2027-42.
- Aman TK**, Raman IM. Inwardly permeating Na ions generate the voltage dependence of resurgent Na current in cerebellar Purkinje neurons. *J Neurosci.* 2010 Apr 21;30(16):5629-34.
- Amatniek JC**, Hauser WA, DelCastillo-Castaneda C, Jacobs DM, Marder K, Bell K, Albert M, Brandt J, Stern Y. Incidence and predictors of seizures in patients with Alzheimer's disease. *Epilepsia.* 2006 May;47(5):867-72.
- Bähler M**, Rhoads A. Calmodulin signaling via the IQ motif. *FEBS Lett.* 2002 Feb 20;513(1):107-13.
- Bant JS**, Raman IM. Control of transient, resurgent, and persistent current by open-channel block by Na channel beta4 in cultured cerebellar granule neurons. *Proc Natl Acad Sci U S A.* 2010 Jul 6;107(27):12357-62.
- Biskup C**, Zimmer T, Benndorf K. FRET between cardiac Na<sup>+</sup> channel subunits measured with a confocal microscope and a streak camera. *Nat Biotechnol.* 2004 Feb;22(2):220-4.

- Black JA**, Newcombe J, Trapp BD, Waxman SG. Sodium channel expression within chronic multiple sclerosis plaques. *J Neuropathol Exp Neurol.* 2007 Sep;66(9):828-37.
- Boiko T**, Van Wart A, Caldwell JH, Levinson SR, Trimmer JS, Matthews G. Functional specialization of the axon initial segment by isoform-specific sodium channel targeting. *J Neurosci.* 2003 Mar 15;23(6):2306-13.
- Boiko T**, Rasband MN, Levinson SR, Caldwell JH, Mandel G, Trimmer JS, Matthews G. Compact myelin dictates the differential targeting of two sodium channel isoforms in the same axon. *Neuron.* 2001 Apr;30(1):91-104.
- Brackenbury WJ**, Calhoun JD, Chen C, Miyazaki H, Nukina N, Oyama F, Ranscht B, Isom LL. Functional reciprocity between Na<sup>+</sup> channel Nav1.6 and beta1 subunits in the coordinated regulation of excitability and neurite outgrowth. *Proc Natl Acad Sci U S A.* 2010 Feb 2;107(5):2283-8.
- Brackenbury WJ**, Isom LL. Na Channel  $\beta$  Subunits: Overachievers of the Ion Channel Family. *Front Pharmacol.* 2011 Sep 28;2:53.
- Burgess DL**, Kohrman DC, Galt J, Plummer NW, Jones JM, Spear B, Meisler MH. Mutation of a new sodium channel gene, Scn8a, in the mouse mutant 'motor endplate disease. *Nat Genet.* 1995 Aug;10(4):461-5.
- Cabrejo L**, Guyant-Maréchal L, Laquerrière A, Vercelletto M, De la Fournière F, Thomas-Antérion C, Verny C, Letournel F, Pasquier F, Vital A, Checler F, Frebourg T, Campion D, Hannequin D. Phenotype associated with APP duplication in five families. *Brain.* 2006 Nov;129(Pt 11):2966-76.
- Caldwell JH**, Schaller KL, Lasher RS, Peles E, Levinson SR. Sodium channel Na(v)1.6 is localized at nodes of ranvier, dendrites, and synapses. *Proc Natl Acad Sci U S A.* 2000 May 9;97(10):5616-20

- Cannon SC**, Bean BP. Sodium channels gone wild: resurgent current from neuronal and muscle channelopathies. *J Clin Invest.* 2010 Jan;120(1):80-3.
- Catterall WA** From ionic currents to molecular mechanisms: the structure and function of voltage-gated sodium channels. *Neuron.* 2000 Apr;26(1):13-25. *Review.*
- Catterall WA**, Perez-Reyes E, Snutch TP, Striessnig J. International Union of Pharmacology. XLVIII. Nomenclature and structure-function relationships of voltage-gated calcium channels. *Pharmacol Rev.* 2005 Dec;57(4):411-25. *Review.*
- Chen Y**, Yu L, Qin SM Detection of subthreshold pulses in neurons with channel noise. *Phys Rev E Stat Nonlin Soft Matter Phys.* 2008 Nov;78(5 Pt 1):051909.
- Chen YH**, Dale TJ, Romanos MA, Whitaker WR, Xie XM, Clare JJ. Cloning, distribution and functional analysis of the type III sodium channel from human brain. *Eur J Neurosci.* 2000 Dec;12(12):4281-9.
- Cheung H**, Kamp D, Harris E. An in vitro investigation of the action of lamotrigine on neuronal voltage-activated sodium channels. *Epilepsy Res.* 1992 Nov;13(2):107-12.
- Chin J**, Palop JJ, Puoliväli J, Massaro C, Bien-Ly N, Gerstein H, Scarce-Lavie K, Masliah E, Mucke L. Fyn kinase induces synaptic and cognitive impairments in a transgenic mouse model of Alzheimer's disease. *J Neurosci.* 2005 Oct 19;25(42):9694-703
- Chin J**, Palop JJ, Yu GQ, Kojima N, Masliah E, Mucke L. Fyn kinase modulates synaptotoxicity, but not aberrant sprouting, in human amyloid precursor protein transgenic mice. *J Neurosci.* 2004 May 12;24(19):4692-7.
- Chiu SY**, Schragger P, Ritchie JM Neuronal-type Na<sup>+</sup> and K<sup>+</sup> channels in rabbit cultured Schwann cells. *Nature.* 1984 Sep 13-19;311(5982):156-7.

- Citron M.** Strategies for disease modification in Alzheimer's disease. *Nat Rev Neurosci.* 2004 Sep;5(9):677-85. Review.
- Cleary JP,** Walsh DM, Hofmeister JJ, Shankar GM, Kuskowski MA, Selkoe DJ, Ashe KH Natural oligomers of the amyloid-beta protein specifically disrupt cognitive function. *Nat Neurosci.* 2005 Jan;8(1):79-84.
- Corbett BF,** Leiser SC, Ling HP, Nagy R, Breysse N, Zhang X, Hazra A, Brown JT, Randall AD, Wood A, Pangalos MN, Reinhart PH, Chin J. Sodium channel cleavage is associated with aberrant neuronal activity and cognitive deficits in a mouse model of Alzheimer's disease. *J Neurosci.* 2013 Apr 17;33(16):7020-6.
- Craner MJ,** Newcombe J, Black JA, Hartle C, Cuzner ML, Waxman SG. Molecular changes in neurons in multiple sclerosis: altered axonal expression of Nav1.2 and Nav1.6 sodium channels and Na<sup>+</sup>/Ca<sup>2+</sup> exchanger. *Proc Natl Acad Sci U S A.* 2004 May 25;101(21):8168-73
- Craner MJ,** Damarjian TG, Liu S, Hains BC, Lo AC, Black JA, Newcombe J, Cuzner ML, Waxman SG. Sodium channels contribute to microglia/macrophage activation and function in EAE and MS. *Glia.* 2005 Jan 15;49(2):220-9.
- Crill WE.** Persistent sodium current in mammalian central neurons. *Annu Rev Physiol.* 1996;58:349-62.
- Davis JQ,** Lambert S, Bennett V. Molecular composition of the node of Ranvier: identification of ankyrin-binding cell adhesion molecules neurofascin (mucin+/third FNIII domain-) and NrCAM at nodal axon segments. *J Cell Biol.* 1996 Dec;135(5):1355-67.
- DeKosky ST,** Scheff SW. Synapse loss in frontal cortex biopsies in Alzheimer's disease: correlation with cognitive severity. *Ann Neurol.* 1990 May;27(5):457-64.

- Deschênes I**, Neyroud N, DiSilvestre D, Marbán E, Yue DT, Tomaselli GF. Isoform-specific modulation of voltage-gated Na(+) channels by calmodulin. *Circ Res.* 2002 Mar 8;**90(4):E49-57.**
- Dib-Hajj SD**, Waxman SG Isoform-specific and pan-channel partners regulate trafficking and plasma membrane stability; and alter sodium channel gating properties. *Neurosci Lett.* 2010 Dec 10;**486(2):84-91. Review.**
- Estacion M**, O'Brien JE, Conravey A, Hammer MF, Waxman SG, Dib-Hajj SD, Meisler MH. A novel de novo mutation of SCN8A (Nav1.6) with enhanced channel activation in a child with epileptic encephalopathy. *Neurobiol Dis.* 2014 Sep;**69:117-23.**
- Feldkamp MD**, Yu L, Shea MA. Structural and energetic determinants of apo calmodulin binding to the IQ motif of the Na(V)1.2 voltage-dependent sodium channel. *Structure.* 2011 May 11;**19(5):733-47.**
- Fotia AB**, Ekberg J, Adams DJ, Cook DI, Poronnik P, Kumar S. Regulation of neuronal voltage-gated sodium channels by the ubiquitin-protein ligases Nedd4 and Nedd4-2. *J Biol Chem.* 2004 Jul 9;**279(28):28930-5.**
- French CR**, Sah P, Buckett KJ, Gage PW. A voltage-dependent persistent sodium current in mammalian hippocampal neurons. *J Gen Physiol.* 1990 Jun;**95(6):1139-57.**
- Games D**, Adams D, Alessandrini R, Barbour R, Berthelette P, Blackwell C, Carr T, Clemens J, Donaldson T, Gillespie F, et al. Alzheimer-type neuropathology in transgenic mice overexpressing V717F beta-amyloid precursor protein. *Nature.* 1995 Feb 9;**373(6514):523-7.**
- Gasser A**, Cheng X, Gilmore ES, Tyrrell L, Waxman SG, Dib-Hajj SD. Two Nedd4-binding motifs underlie modulation of sodium channel Nav1.6 by p38 MAPK. *J Biol Chem.* 2010 Aug 20;**285(34):26149-61.**
- Gasser A**, Ho TS, Cheng X, Chang KJ, Waxman SG, Rasband MN, Dib-Hajj SD An ankyrinG-binding motif is necessary and sufficient for targeting

- Nav1.6 sodium channels to axon initial segments and nodes of Ranvier. **J Neurosci.** 2012 May 23;32(21):7232-43.
- Glennner GG**, Wong CW Alzheimer's disease: initial report of the purification and characterization of a novel cerebrovascular amyloid protein. **Biochem Biophys Res Commun.** 1984 May 16;120(3):885-90
- Gordienko DV**, Tsukahara H Tetrodotoxin-blockable depolarization-activated Na<sup>+</sup> currents in a cultured endothelial cell line derived from rat interlobar arter and human umbilical vein. **Pflugers Arch.** 1994 Aug;428(1):91-3.
- Götz J**, Schild A, Hoerndli F, Pennanen L Amyloid-induced neurofibrillary tangle formation in Alzheimer's disease: insight from transgenic mouse and tissue-culture models. **Int J Dev Neurosci.** 2004 Nov;22(7):453-65.  
*Review.*
- Greenfield JP**, Tsai J, Gouras GK, Hai B, Thinakaran G, Checler F, Sisodia SS, Greengard P, Xu H. Endoplasmic reticulum and trans-Golgi network generate distinct populations of Alzheimer beta-amyloid peptides. **Proc Natl Acad Sci U S A.** 1999 Jan 19;96(2):742-7.
- Grieco TM**, Malhotra JD, Chen C, Isom LL, Raman IM. Open-channel block by the cytoplasmic tail of sodium channel beta4 as a mechanism for resurgent sodium current. **Neuron.** 2005 Jan 20;45(2):233-44.
- Guo X**, Wu X, Ren L, Liu G, Li L. Epigenetic mechanisms of amyloid- $\beta$  production in anisomycin-treated SH-SY5Y cells. **Neuroscience.** 2011 Oct 27;194:272-8.
- Harris JA**, Devidze N, Verret L, Ho K, Halabisky B, Thwin MT, Kim D, Hamto P, Lo I, Yu GQ, Palop JJ, Masliah E, Mucke L Transsynaptic progression of amyloid- $\beta$ -induced neuronal dysfunction within the entorhinal-hippocampal network. **Neuron.** 2010 Nov 4;68(3):428-41.
- Hauser WA**, Morris ML, Heston LL, Anderson VE Seizures and myoclonus in patients with Alzheimer's disease. **Neurology.** 1986 Sep;36(9):1226-30.

- Herzog RI**, Liu C, Waxman SG, Cummins TR. Calmodulin binds to the C terminus of sodium channels Nav1.4 and Nav1.6 and differentially modulates their functional properties. *J Neurosci.* 2003 Sep 10;23(23):8261-70.
- Hesdorffer DC**, Hauser WA, Annegers JF, Kokmen E, Rocca WA. Dementia and adult-onset unprovoked seizures. *Neurology.* 1996 Mar;46(3):727-30.
- Hill AS**, Nishino A, Nakajo K, Zhang G, Fineman JR, Selzer ME, Okamura Y, Cooper EC. Ion channel clustering at the axon initial segment and node of Ranvier evolved sequentially in early chordates. *PLoS Genet.* 2008 Dec;4(12).
- Hsiao K**, Chapman P, Nilsen S, Eckman C, Harigaya Y, Younkin S, Yang F, Cole G Correlative memory deficits, Abeta elevation, and amyloid plaques in transgenic mice. *Science.* 1996 Oct 4;274(5284):99-102.
- Hsiao KK**, Borchelt DR, Olson K, Johannsdottir R, Kitt C, Yunis W, Xu S, Eckman C, Younkin S, Price D, et al. Age-related CNS disorder and early death in transgenic FVB/N mice overexpressing Alzheimer amyloid precursor proteins. *Neuron.* 1995 Nov;15(5):1203-18.
- Hu W**, Tian C, Li T, Yang M, Hou H, Shu Y. Distinct contributions of Na(v)1.6 and Na(v)1.2 in action potential initiation and backpropagation. *Nat Neurosci.* 2009 Aug;12(8):996-1002.
- Ingham RJ**, Gish G, Pawson T. The Nedd4 family of E3 ubiquitin ligases: functional diversity within a common modular architecture. *Oncogene.* 2004 Mar 15;23(11):1972-84.
- Isom LL**. Beta subunits: players in neuronal hyperexcitability? *Novartis Found Symp.* 2002;241:124-38; discussion 138-43, 226-32. Review.
- Isom LL**. Sodium channel beta subunits: anything but auxiliary. *Neuroscientist.* 2001 Feb;7(1):42-54. Review.

- Jarnot MD**, Corbett AM. High titer antibody to mammalian neuronal sodium channels produces sustained channel block. *Brain Res.* 1995 Mar 13;674(1):159-62.
- Jarrett JT**, Berger EP, Lansbury PT Jr. The C-terminus of the beta protein is critical in amyloidogenesis. *Ann N Y Acad Sci.* 1993 Sep 24;695:144-8. *Review.*
- Kaplan MR**, Cho MH, Ullian EM, Isom LL, Levinson SR, Barres BA. Differential control of clustering of the sodium channels Na(v)1.2 and Na(v)1.6 at developing CNS nodes of Ranvier. *Neuron.* 2001 Apr;30(1):105-19.
- Kearney JA**, Buchner DA, De Haan G, Adamska M, Levin SI, Furay AR, Albin RL, Jones JM, Montal M, Stevens MJ, Sprunger LK, Meisler MH. Molecular and pathological effects of a modifier gene on deficiency of the sodium channel Scn8a (Na(v)1.6). *Hum Mol Genet.* 2002 Oct 15;11(22):2765-75.
- Kim DY**, Carey BW, Wang H, Ingano LA, Binshtok AM, Wertz MH, Pettingell WH, He P, Lee VM, Woolf CJ, Kovacs DM. BACE1 regulates voltage-gated sodium channels and neuronal activity. *Nat Cell Biol.* 2007 Jul;9(7):755-64.
- Kobayashi DT**, Chen KS Behavioral phenotypes of amyloid-based genetically modified mouse models of Alzheimer's disease. *Genes Brain Behav.* 2005 Apr;4(3):173-96.
- Krzemien DM**, Schaller KL, Levinson SR, Caldwell JH. Immunolocalization of sodium channel isoform NaCh6 in the nervous system. *J Comp Neurol.* 2000 Apr 24;420(1):70-83.
- LaFerla FM**, Tinkle BT, Bieberich CJ, Haudenschild CC, Jay G. The Alzheimer's A beta peptide induces neurodegeneration and apoptotic cell death in transgenic mice. *Nat Genet.* 1995 Jan;9(1):21-30.

- Lalonde R**, Dumont M, Staufenbiel M, Strazielle C. Neurobehavioral characterization of APP23 transgenic mice with the SHIRPA primary screen. *Behav Brain Res.* 2005 Feb 10;157(1):91-8.
- Larner AJ**, Doran M. Clinical phenotypic heterogeneity of Alzheimer's disease associated with mutations of the presenilin-1 gene. *J Neurol.* 2006 Feb;253(2):139-58. *Review.*
- Lemaillet G**, Walker B, Lambert S. Identification of a conserved ankyrin-binding motif in the family of sodium channel alpha subunits. *J Biol Chem.* 2003 Jul 25;278(30):27333-9.
- Levin SI**, Khaliq ZM, Aman TK, Grieco TM, Kearney JA, Raman IM, Meisler MH. Impaired motor function in mice with cell-specific knockout of sodium channel Scn8a (NaV1.6) in cerebellar purkinje neurons and granule cells. *J Neurophysiol.* 2006 Aug;96(2):785-93.
- Levin SI**, Khaliq ZM, Aman TK, Grieco TM, Kearney JA, Raman IM, Meisler MH. Impaired motor function in mice with cell-specific knockout of sodium channel Scn8a (NaV1.6) in cerebellar purkinje neurons and granule cells. *J Neurophysiol.* 2006 Aug;96(2):785-93.
- Lim AC**, Qi RZ. Cyclin-dependent kinases in neural development and degeneration. *J Alzheimers Dis.* 2003 Aug;5(4):329-35.
- Lorenzo A**, Yankner BA. Beta-amyloid neurotoxicity requires fibril formation and is inhibited by congo red. *Proc Natl Acad Sci U S A.* 1994 Dec 6;91(25):12243-7.
- Lorincz A**, Nusser Z. Cell-type-dependent molecular composition of the axon initial segment. *J Neurosci.* 2008 Dec 31;28(53):14329-40.
- Lorincz A**, Nusser Z. Molecular identity of dendritic voltage-gated sodium channels. *Science.* 2010 May 14;328(5980):906-9.

- Lozsadi DA**, Lerner AJ. Prevalence and causes of seizures at the time of diagnosis of probable Alzheimer's disease. *Dement Geriatr Cogn Disord.* 2006;22(2):121-4.
- Ma JY**, Catterall WA, Scheuer T. Persistent sodium currents through brain sodium channels induced by G protein beta gamma subunits. *Neuron.* 1997 Aug;19(2):443-52.
- Magistretti J, Alonso A.** Biophysical properties and slow voltage-dependent inactivation of a sustained sodium current in entorhinal cortex layer-II principal neurons: a whole-cell and single-channel study. *J Gen Physiol.* 1999 Oct;114(4):491-509.
- Maltsev VA**, Reznikov V, Undrovinas NA, Sabbah HN, Undrovinas A. Modulation of late sodium current by Ca<sup>2+</sup>, calmodulin, and CaMKII in normal and failing dog cardiomyocytes: similarities and differences. *Am J Physiol Heart Circ Physiol.* 2008 Apr;294(4):H1597-608.
- Martin MS**, Tang B, Papale LA, Yu FH, Catterall WA, Escayg A. The voltage-gated sodium channel Scn8a is a genetic modifier of severe myoclonic epilepsy of infancy. *Hum Mol Genet.* 2007 Dec 1;16(23):2892-9.
- Maurice N**, Tkatch T, Meisler M, Sprunger LK, Surmeier DJ. D1/D5 dopamine receptor activation differentially modulates rapidly inactivating and persistent sodium currents in prefrontal cortex pyramidal neurons. *J Neurosci.* 2001 Apr 1;21(7):2268-77.
- McCormick KA**, Isom LL, Ragsdale D, Smith D, Scheuer T, Catterall WA. Molecular determinants of Na<sup>+</sup> channel function in the extracellular domain of the beta1 subunit. *J Biol Chem.* 1998 Feb 13;273(7):3954-62.
- McKinney BC**, Chow CY, Meisler MH, Murphy GG. Exaggerated emotional behavior in mice heterozygous null for the sodium channel Scn8a (Nav1.6). *Genes Brain Behav.* 2008 Aug;7(6):629-38.
- Meisler MH**, Kearney JA, Sprunger LK, MacDonald BT, Buchner DA, Escayg A. Mutations of voltage-gated sodium channels in movement disorders

and epilepsy. *Novartis Found Symp.* 2002;241:72-81; discussion 82-6, 226-32. Review.

**Meisler MH**, Plummer NW, Burgess DL, Buchner DA, Sprunger LK. Allelic mutations of the sodium channel SCN8A reveal multiple cellular and physiological functions. *Genetica.* 2004 Sep;122(1):37-45. Review.

**Mendez MF**, Clark DG, Shapira JS, Cummings JL Speech and language in progressive nonfluent aphasia compared with early Alzheimer's disease. *Neurology.* 2003 Oct 28;61(8):1108-13.

**Mendez MF**, Catanzaro P, Doss RC, ARguello R, Frey WH 2nd Seizures in Alzheimer's disease: clinicopathologic study. *J Geriatr Psychiatry Neurol.* 1994 Oct-Dec;7(4):230-3

**Minkeviciene R**, Rheims S, Dobszay MB, Zilberter M, Hartikainen J, Fülöp L, Penke B, Zilberter Y, Harkany T, Pitkänen A, Tanila H Amyloid beta-induced neuronal hyperexcitability triggers progressive epilepsy. *J Neurosci.* 2009 Mar 18;29(11):3453-62.

**Moechars D**, Dewachter I, Lorent K, Reversé D, Baekelandt V, Naidu A, Tesseur I, Spittaels K, Haute CV, Checler F, Godaux E, Cordell B, Van Leuven F Early phenotypic changes in transgenic mice that overexpress different mutants of amyloid precursor protein in brain. *J Biol Chem.* 1999 Mar 5;274(10):6483-92.

**Mori M**, Konno T, Morii T, Nagayama K, Imoto K Regulatory interaction of sodium channel IQ-motif with calmodulin C-terminal lobe. *Biochem Biophys Res Commun.* 2003 Jul 25;307(2):290-6.

**Mukhamedyarov MA**, Grishin SN, Yusupova ER, Zefirov AL, Palotas A. Alzheimer's  $\beta$ -Amyloid-induced depolarization of skeletal muscle fibers: implications for motor dysfunctions in dementia. *Cell Physiol Biochem* 2009;23:109-114.

**O'Brien JE**, Sharkey LM, Vallianatos CN, Han C, Blossom JC, Yu T, Waxman SG, Dib-Hajj SD, Meisler MH Interaction of voltage-gated sodium channel

- Nav1.6 (SCN8A) with microtubule-associated protein Map1b. *J Biol Chem.* 2012 May 25;287(22):18459-66.
- Palop JJ**, Chin J, Bien-Ly N, Massaro C, Yeung BZ, Yu GQ, Mucke L. Vulnerability of dentate granule cells to disruption of arc expression in human amyloid precursor protein transgenic mice. *J Neurosci.* 2005 Oct 19;25(42):9686-93
- Palop JJ**, Chin J, Roberson ED, Wang J, Thwin MT, Bien-Ly N, Yoo J, Ho KO, Yu GQ, Kreitzer A, Finkbeiner S, Noebels JL, Mucke L. Aberrant excitatory neuronal activity and compensatory remodeling of inhibitory hippocampal circuits in mouse models of Alzheimer's disease. *Neuron.* 2007 Sep 6;55(5):697-711.
- Palop JJ**, Jones B, Kekoni L, Chin J, Yu GQ, Raber J, Masliah E, Mucke L. Neuronal depletion of calcium-dependent proteins in the dentate gyrus is tightly linked to Alzheimer's disease-related cognitive deficits. *Proc Natl Acad Sci U S A.* 2003 Aug 5;100(16):9572-7.
- Palop JJ**, Mucke L. Epilepsy and cognitive impairments in Alzheimer disease. *Arch Neurol.* 2009 Apr;66(4):435-40. *Review.*
- Pannaccione A**, Secondo A, Molinaro P, D'Avanzo C, Cantile M, Esposito A, Boscia F, Scorziello A, Sirabella R, Sokolow S, Herchuelz A, Di Renzo G, Annunziato L. A new concept: A $\beta$ 1-42 generates a hyperfunctional proteolytic NCX3 fragment that delays caspase-12 activation and neuronal death. *J Neurosci.* 2012 Aug 1;32(31):10609-17. Erratum in: *J Neurosci.* 2012 Dec 12;32(50):18269. Sokolow, Sophie [added]; Herchuelz, André [added].
- Patino GA**, Isom LL. Electrophysiology and beyond: multiple roles of Na<sup>+</sup> channel  $\beta$  subunits in development and disease. *Neurosci Lett.* 2010 Dec 10;486(2):53-9.
- Plummer NW**, Galt J, Jones JM, Burgess DL, Sprunger LK, Kohrman DC, Meisler MH. Exon organization, coding sequence, physical mapping, and

polymorphic intragenic markers for the human neuronal sodium channel gene SCN8A. **Genomics. 1998 Dec 1;54(2):287-96.**

**Qu Y**, Curtis R, Lawson D, Gilbride K, Ge P, DiStefano PS, Silos-Santiago I, Catterall WA, Scheuer T Differential modulation of sodium channel gating and persistent sodium currents by the beta1, beta2, and beta3 subunits. **Mol Cell Neurosci. 2001 Nov;18(5):570-80.**

**Rabinowicz AL**, Starkstein SE, Leiguarda RC, Coleman AE Transient epileptic amnesia in dementia: a treatable unrecognized cause of episodic amnesic wandering. **Alzheimer Dis Assoc Disord. 2000 Oct-Dec;14(4):231-3.**

**Raman IM**, Sprunger LK, Meisler MH, Bean BP. Altered subthreshold sodium currents and disrupted firing patterns in Purkinje neurons of Scn8a mutant mice. **Neuron. 1997 Oct;19(4):881-91.**

**Raman IM**, Bean BP Resurgent sodium current and action potential formation in dissociated cerebellar Purkinje neurons. **J Neurosci. 1997 Jun 15;17(12):4517-26.**

**Ren SC**, Chen PZ, Jiang HH, Mi Z, Xu F, Hu B, Zhang J, Zhu ZR. Persistent sodium currents contribute to A $\beta$ 1-42-induced hyperexcitation of hippocampal CA1 pyramidal neurons. **Neurosci Lett. 2014 Sep 19;580:62-7.**

**Riederer BM**. Microtubule-associated protein 1B, a growth-associated and phosphorylated scaffold protein. **Brain Res Bull. 2007 Mar 30;71(6):541-58. Review.**

**Roberson ED**, Halabisky B, Yoo JW, Yao J, Chin J, Yan F, Wu T, Hamto P, Devidze N, Yu GQ, Palop JJ, Noebels JL, Mucke L Amyloid- $\beta$ /Fyn-induced synaptic, network, and cognitive impairments depend on tau levels in multiple mouse models of Alzheimer's disease. **J Neurosci. 2011 Jan 12;31(2):700-11.**

- Rush AM**, Dib-Hajj SD, Waxman SG. Electrophysiological properties of two axonal sodium channels, Nav1.2 and Nav1.6, expressed in mouse spinal sensory neurons. *J Physiol.* 2005 May 1;**564(Pt 3):803-15.**
- Sanchez PE**, Zhu L, Verret L, Vossel KA, Orr AG, Cirrito JR, Devidze N, Ho K, Yu GQ, Palop JJ, Mucke L. Levetiracetam suppresses neuronal network dysfunction and reverses synaptic and cognitive deficits in an Alzheimer's disease model. *Proc Natl Acad Sci U S A.* 2012 Oct 16;**109(42):E2895-903.**
- Schaller KL**, Caldwell JH. Developmental and regional expression of sodium channel isoform NaCh6 in the rat central nervous system. *J Comp Neurol.* 2000 Apr 24;**420(1):84-97.**
- Selkoe DJ.** The genetics and molecular pathology of Alzheimer's disease: roles of amyloid and the presenilins. *Neurol Clin.* 2000 Nov;**18(4):903-22. Review.**
- Smith MR**, Smith RD, Plummer NW, Meisler MH, Goldin AL. Functional analysis of the mouse Scn8a sodium channel. *J Neurosci.* 1998 Aug 15;**18(16):6093-102.**
- Snider BJ**, Norton J, Coats MA, Chakraverty S, Hou CE, Jervis R, Lendon CL, Goate AM, McKeel DW Jr, Morris JC Novel presenilin 1 mutation (S170F) causing Alzheimer disease with Lewy bodies in the third decade of life. *Arch Neurol.* 2005 Dec;**62(12):1821-30.**
- Spampanato J**, Escayg A, Meisler MH, Goldin AL. Functional effects of two voltage-gated sodium channel mutations that cause generalized epilepsy with febrile seizures plus type 2. *J Neurosci.* 2001 Oct 1;**21(19):7481-90.**
- Spampanato J**, Kearney JA, de Haan G, McEwen DP, Escayg A, Aradi I, MacDonald BT, Levin SI, Soltesz I, Benna P, Montalenti E, Isom LL, Goldin AL, Meisler MH. A novel epilepsy mutation in the sodium channel SCN1A identifies a cytoplasmic domain for beta subunit interaction. *J Neurosci.* 2004 Nov 3;**24(44):10022-34.**

- Srinivasan Y**, Elmer L, Davis J, Bennett V, Angelides K. Ankyrin and spectrin associate with voltage-dependent sodium channels in brain. *Nature*. 1988 May 12;333(6169):177-80.
- Stühmer W**, Conti F, Suzuki H, Wang XD, Noda M, Yahagi N, Kubo H, Numa S. Structural parts involved in activation and inactivation of the sodium channel. *Nature*. 1989 Jun 22;339(6226):597-603.
- Sudol M, Hunter T** New wrinkles for an old domain. *Cell*. 2000 Dec 22;103(7):1001-4.
- Tanzi RE**, Bertram L. Twenty years of the Alzheimer's disease amyloid hypothesis: a genetic perspective. *Cell*. 2005 Feb 25;120(4):545-55.  
*Review*
- Terlau H**, Stühmer W. Structure and function of voltage-gated ion channels. *Naturwissenschaften*. 1998 Sep;85(9):437-44.
- Trudeau MM**, Dalton JC, Day JW, Ranum LP, Meisler MH. Heterozygosity for a protein truncation mutation of sodium channel SCN8A in a patient with cerebellar atrophy, ataxia, and mental retardation. *J Med Genet*. 2006 Jun;43(6):527-30.
- Van Wart A**, Matthews G. Impaired firing and cell-specific compensation in neurons lacking nav1.6 sodium channels. *J Neurosci*. 2006 Jul 5;26(27):7172-80.
- Van Wart A**, Trimmer JS, Matthews G. Polarized distribution of ion channels within microdomains of the axon initial segment. *J Comp Neurol*. 2007 Jan 10;500(2):339-52.
- Van Wart A**, Matthews G. Expression of sodium channels Nav1.2 and Nav1.6 during postnatal development of the retina. *Neurosci Lett*. 2006 Aug 7;403(3):315-7.
- Veeramah KR**, O'Brien JE, Meisler MH, Cheng X, Dib-Hajj SD, Waxman SG, Talwar D, Girirajan S, Eichler EE, Restifo LL, Erickson RP, Hammer

- MF De novo pathogenic SCN8A mutation identified by whole-genome sequencing of a family quartet affected by infantile epileptic encephalopathy and SUDEP. *Am J Hum Genet.* 2012 Mar 9;90(3):502-10.
- Verret L**, Mann EO, Hang GB, Barth AM, Cobos I, Ho K, Devidze N, Masliah E, Kreitzer AC, Mody I, Mucke L, Palop JJ. Inhibitory interneuron deficit links altered network activity and cognitive dysfunction in Alzheimer model. *Cell.* 2012 Apr 27;149(3):708-21.
- Vogt DL**, Thomas D, Galvan V, Bredesen DE, Lamb BT, Pimplikar SW. Abnormal neuronal networks and seizure susceptibility in mice overexpressing the APP intracellular domain. *Neurobiol Aging.* 2011 Sep;32(9):1725-9.
- Walsh DM**, Selkoe DJ Deciphering the molecular basis of memory failure in Alzheimer's disease. *Neuron.* 2004 Sep 30;44(1):181-93. Review
- Whitaker WR**, Faull RL, Waldvogel HJ, Plumpton CJ, Emson PC, Clare JJ. Comparative distribution of voltage-gated sodium channel proteins in human brain. *Brain Res Mol Brain Res.* 2001 Mar 31;88(1-2):37-53.
- Wittmack EK**, Rush AM, Hudmon A, Waxman SG, Dib-Hajj SD. Voltage-gated sodium channel Nav1.6 is modulated by p38 mitogen-activated protein kinase. *J Neurosci.* 2005 Jul 13;25(28):6621-30.
- Wong HK**, Sakurai T, Oyama F, Kaneko K, Wada K, Miyazaki H, Kurosawa M, De Strooper B, Saftig P, Nukina N beta Subunits of voltage-gated sodium channels are novel substrates of beta-site amyloid precursor protein-cleaving enzyme (BACE1) and gamma-secretase. *J Biol Chem.* 2005 Jun 17;280(24):23009-17.
- Yankner BA**, Dawes LR, Fisher S, Villa-Komaroff L, Oster-Granite ML, Neve RL. Neurotoxicity of a fragment of the amyloid precursor associated with Alzheimer's disease. *Science.* 1989 Jul 28;245(4916):417-20.

**Yarov-Yarovoy V**, DeCaen PG, Westenbroek RE, Pan CY, Scheuer T, Baker D, Catterall WA Structural basis for gating charge movement in the voltage sensor of a sodium channel. *Proc Natl Acad Sci U S A*. 2012 Jan 10;109(2).

**Yu FH, Catterall WA** The VGL-kanome: a protein superfamily specialized for electrical signaling and ionic homeostasis. *Sci STKE*. 2004 Oct 5;2004(253):re15.

**Yu FH, Catterall WA**. Overview of the voltage-gated sodium channel family. *Genome Biol*. 2003;4(3):207. Review.

**Zarrinpar A, Lim WA** Converging on proline: the mechanism of WW domain peptide recognition. *Nat Struct Biol*. 2000 Aug;7(8):611-3.

**Ziyatdinova S**, Gurevicius K, Kutchiashvili N, Bolkvadze T, Nissinen J, Tanila H, Pitkänen A. Spontaneous epileptiform discharges in a mouse model of Alzheimer's disease are suppressed by antiepileptic drugs that block sodium channels. *Epilepsy Res*. 2011 Mar;94(1-2):75-85.